Adaptation and mitigation of pollution: Evidence from air quality warnings

Sandra Aguilar-Gomez *

August 11, 2025

Abstract

Many cities have adopted air quality alert systems to reduce the health risks from severe pollution episodes, pairing public messaging with temporary restrictions on vehicle and industrial activity. Despite their widespread implementation, evidence on their effectiveness remains mixed, in part because of data limitations and a focus on traffic-only or voluntary measures. This paper evaluates Mexico City's air quality alert program using a fuzzy regression discontinuity design that exploits a preset ozone threshold for policy activation. I find that alerts lead to significant improvements in ozone and sulfur dioxide concentrations and sizable reductions in emergency department visits for respiratory (56% decrease) and cardiovascular conditions (50% decrease). The effects on transport-related pollutants are smaller and time-dependent, consistent with the alerts mitigating vehicle emissions more slowly. To assess mechanisms, I analyze information-seeking behavior, mobility data, and emissions inventories. The alerts increase online searches about air quality and the policy itself, but not about protective behaviors. Traffic volume falls and congestion improves, though public transit usage does not increase. Finally, I show that the pollution reductions are largest near restricted industrial facilities, which suggests that industrial curbs play a central role in policy effectiveness. These results can support the design of short-term environmental response policies in cities facing both mobile and stationary sources of pollution.

Keywords: Pollution control, public health, driving restrictions, air quality warnings, Mexico
JEL Codes: Q50, Q52, Q58, R41, I18

*Tecnologico de Monterrey, Mexico City, Mexico. I thank Jeffrey Shrader, Rodrigo Soares, Sandra Black, Matt Neidell, Lucas Davis, and Eric Verhoogen for their helpful comments and suggestions. I am also grateful to seminar participants at Columbia University, University of Southern California, NBER SI, LSE Workshop in Environmental Economics, Online Summer Workshop in Environment, Energy, and Transportation (OSWEET) and Universidad de los Andes for providing helpful feedback. Maria Jose Cota Acosta and Daniel Perez provided excellent research assistance. Jorge Rodriguez-Arenas provided exceptional research assistance. I thank Samantha Eyler-Driscoll for her support in editing the manuscript. This project received funding from the Center of Environmental Economics and Policy at Columbia University and the Earth Institute. I declare no conflict of interest.

1 Introduction

Standard economic analyses of environmental policy typically focus on two goals: reducing externalities through mitigation or minimizing their harms by promoting adaptation. The former efforts aim to reduce the environmental impacts from human activities, while the latter seek to minimize damages at a given level of environmental degradation through protective behavior. Limiting emissions of hazardous particles is a classic mitigation strategy, and information provision is a common response aimed at facilitating adaptation. In practice, both strategies are critical, given the health and economic costs of local air pollutants, which can be acute.[1]

While navigating the political complexities of implementing long-run air pollution solutions, city governments worldwide have increasingly adopted air quality warnings to reduce the health impacts of days with very high pollution. These programs are especially relevant in regions where extreme pollution episodes result from rapid urbanization, often characterized by inadequate planning and weak environmental oversight. In many such contexts, car-oriented investments have incentivized the growth of a bloated vehicle fleet and notorious traffic congestion, while industrial zones remain embedded within residential and commercial areas, with urban design offering few protections from pollution exposure. Air quality warnings released when pollution passes a certain threshold inform people about the risks of going outdoors and encourage them to reduce their exposure to hazardous air quality. Many cities' air quality response systems include temporary restrictions, usually on transport emissions, to mitigate outdoor air pollutants. In some cities, including Mexico City, Santiago, Delhi and Beijing, these programs also restrict—to different extents—industrial and power generating facilities within their metropolitan area (Li et al., 2023b; Mullins and Bharadwaj, 2015; Singh and Kulshrestha, 2020).

In this paper, I examine the causal effects of the Mexico City Environmental Alerts Program (PCAA,[2] its acronym in Spanish). Since 2016, the program has combined intensive public messaging with mandatory driving restrictions affecting over half of the city's private vehicles and legally binding limits on industrial operations imposing activity reductions of up to 50% in most industrial facilities within the metropolitan area. To causally identify the impacts of air quality warnings, I exploit the PCAA's reliance on an arbitrary ozone-based cutoff as a trigger for the alerts. Mexico City's regulatory framework is complemented

[1] See Aguilar-Gomez and Rivera (2024) and Aguilar-Gomez et al. (2022) for reviews of studies on the health and nonhealth effects of pollution, respectively.

[2] Programa de Contingencias Ambientales y Atmosféricas.

by a dense real-time monitoring network (SIMAT), an annual emissions inventory, and a mandatory pollutant-release transfer register (RETC). I leverage these data sources and institutional setting to implement a regression discontinuity design (RDD), which relies on the assumption of no sharp discontinuities in relevant covariates around the alert threshold.

The policy generates strong same-day reductions in the target pollutant, ozone: The intention-to-treat (ITT) effect of -22.7 parts per billion (ppb) represents nearly 75% of the sample mean of 31 ppb. The hourly local average treatment effect (LATE) estimates indicate that reductions in hourly concentration surpass 25 ppb during the afternoon hours. Ozone is not directly emitted but is a secondary pollutant; thus, examining other pollutant-specific reductions can shed light on which of the policy's measures are most effective. First, I find substantial reductions in sulfur dioxide (SO_2), a pollutant whose concentrations are driven mainly by industry emissions, with ITT and LATE estimates indicating a reduction of over 71% from the control mean. Hence, the results reveal that the apparently draconian industry restrictions in fact effectively and swiftly improve air quality.

The effects of the alerts on other pollutants are more nuanced and time-dependent. The LATE estimates suggest that the policy almost doubles average concentrations of nitrogen oxides (NO_x) and carbon monoxide (CO)—both particles driven mainly by vehicle combustion—but these effects are driven by morning spikes that become statistically insignificant or negative in the afternoon. Thus, the results suggest that the policy is slower and less effective in reducing transport emissions despite its incorporation of strong traffic restrictions. Particulate matter (PM)—almost half of the concentrations of which are directly emitted by cars, with concentrations of the pollutant aggravated by dust resuspension on unpaved roads—also declines substantially in the second part of the day, with the LATE estimates indicating reductions of over 50%.

To estimate the policy's impacts on health, I employ emergency department (ED) records from public hospitals in the city, focusing on respiratory and cardiovascular admissions across all age groups, with particular attention to vulnerable populations (under five and over 65 years old). For respiratory cases, the ITT and LATE estimates suggest reductions of 3.6 and 4.9 daily visits per hospital, corresponding to 41% and 56% declines relative to the control mean. Among vulnerable groups, the estimated decline ranges between 37% and 50% relative to the control mean. For cardiovascular admissions, I find comparable but less precise results. These results are robust to alternative bandwidth choices and model specifications. As expected, I find no statistically significant effects for outcomes unrelated to short-term exposure to air pollution.

To investigate the channels of the pollution and health improvements, I use four data sources: an awareness measure constructed from Google search data, a novel dataset of car counts and speed measurements from over 300 traffic sensors installed throughout Mexico City, public transportation administrative records, and plant-level emissions reports from the Registro de Emisiones y Transferencia de Contaminantes (RETC).

First, the health improvements described above may be driven by individuals proactively avoiding exposure to pollution upon becoming aware of the air quality warnings. To explore this potential adaptation mechanism, I use a citywide Google search–based awareness index to measure post-alert interest in four topics corresponding to different aspects of adaptive behavior. The findings suggest that the public responses lean more toward information-seeking about air quality and particularly the policy itself, which likely reflects efforts to comply with the driving restrictions. By contrast, there is little indication of heightened interest in pollution-related symptoms or in exposure-avoidance behaviors, such as searching for air purifiers or face masks.

I next analyze mitigation pathways, beginning with reductions in vehicle usage and then turning to industrial emissions. Overall, the results suggest that both reduced mobility and curtailed industrial activity contribute to the observed improvements in air quality and health. The policy leads to a clear reduction in car usage, with decreases in car counts for all vehicle types. While the ITT estimate implies compliance of approximately half (i.e., a 25% decrease in car usage), the LATE confidence interval cannot rule out full compliance. Congestion improves by 4% on alert days, as measured by a roughly 2 km/h increase in average traffic speed. In administrative records on subway, bus rapid transit (BRT), and public bicycle usage, I find no statistically significant changes, though the estimates are negative in sign, possibly reflecting increased stay-at-home behavior counteracting modal shifts. Finally, I link monitor-level SO_2 responses to nearby industrial activity. Using yearly CO_2 emissions reported in the RETC as a proxy for plant-level pollution intensity, I find that monitors closer to high-emitting restricted firms show larger SO_2 reductions, consistent with the alerts curbing emissions from targeted industries.

Broadly, these findings contribute to the information and protective behavior literature and, specifically, the air quality warnings literature, which is focused on the US and Europe, has mostly overlooked programs that include mitigation and has found mixed results on their effectiveness (see Neidell, 2009; Welch et al., 2005; Saberian et al., 2017; Tribby et al., 2013; Dangel and Goeschl, 2025). I extend the frontier by examining the impact of such alerts on information-seeking behavior, industrial emissions, and the ultimate measure of success of a public health policy: reductions in morbidity.

This paper offers lessons for other megacities facing the twofold challenge of ameliorating both industrial and transportation emissions (OECD, 2016; WHO, 2021). Many of these cities are already investing heavily in cleaner vehicles (International Energy Agency, 2024). However, industrial and power generation sources remain substantial contributors to urban pollution, particularly where urban sprawl has enveloped formerly isolated industrial zones and power plants. Several of the programs for managing severe pollution episodes rely primarily on traffic-based or voluntary alert schemes, among them Delhi's Graded Response Action Plan (GRAP) and Jakarta's clean-air alerts, neither of which imposes comprehensive, mandatory industrial curbs.[3] This is despite industry continuing to account for a sizable share of urban SO_2 and primary PM emissions in these regions (Sahu et al., 2023; Lestari et al., 2020; Barraza et al., 2017). By demonstrating that mandatory industrial cuts yield the largest same-day declines in key pollutants (e.g., a 71% drop in SO_2) and sharper improvements near regulated plants, Mexico City's experience highlights a policy gap that other cities could address during pollution emergencies. The high-quality data from the Mexican context also provide relevant insights for cities that do target industry sources in their emergency management programs, such as Santiago in Chile or Beijing in China (Cheng et al., 2017).

My results also help contextualize previous findings from the region and contribute to ongoing debates about the effectiveness of driving restrictions. In Chile, Santiago's environmental episodes program combines temporary limits on both mobile and stationary sources of pollutants and has been shown to generate health benefits (Mullins and Bharadwaj, 2015). While Rivera (2021) attributes these gains to reductions in vehicle use, the role of industrial restrictions—which are part of the policy but applied only during high-alert stages—has not been causally evaluated. My findings suggest that curbing emissions from stationary sources can significantly improve air quality, raising the possibility that the health effects found for Santiago reflect reductions in both traffic and industrial activity. More generally, a related literature has questioned the long-run effectiveness of permanent driving restrictions. In Mexico City, for example, sustained vehicle bans led many households to purchase second, often higher-emitting, cars, offsetting the intended pollution reductions (Davis, 2008; Gallego et al., 2013). Zhang et al. (2017) document similar outcomes in Bogotá. These studies show that, under certain conditions, such as vehicle substitution, changes in transport mode

[3]In Delhi, only at higher tiers (Stages III and IV) does GRAP impose binding restrictions, including construction and demolition bans, suspension of mining activities, closure of stone crushers and, since 2023, shutdown of industries using unauthorized fuels or diesel generators (Anugerah et al., 2021; CAQM, 2022, 2023). In Jakarta, authorities have generally issued voluntary guidance (e.g., advising factories to reduce operations) rather than enforcing industrial shutdowns during smog episodes (Anugerah et al., 2021).

choice, or specific atmospheric responses, license plate–based restrictions can backfire.[4] This paper provides new causal evidence that temporary, binding restrictions, when applied to both vehicles and industry, can yield measurable improvements in air quality and public health.

2 Background

2.1 The PCAA: Measures and implementation

The Mexico City Atmospheric Monitoring System (SIMAT) tracks air pollution concentrations and other meteorological parameters. When pollution levels pose a health risk, the Environmental Commission of the Megalopolis (CAMe) activates a set of mandatory measures to reduce emissions, known as the Environmental and Atmospheric Contingency Program (PCAA). The PCAA combines mitigation and adaptation actions: It disseminates self-protection messages and recommendations to the public while imposing pollution reduction measures on the transport sector, industry, and government activities for the duration of the alert. Table A.1 summarizes the measures in place during the study period (2016–2019). The program has undergone several modifications since its inception in the late 1990s. Although many of these interventions existed on paper before 2016, the activation threshold was substantially lowered in April 2016 to 155 ppb of ozone. Prior to this change, the threshold was so high that the measures were never triggered.[5] Accordingly, I set the start of the analysis period to April 2016 and its end to December 2019 to avoid confounding from COVID-19-related disruptions to mobility and health.[6]

As discussed, the policy has one arm focused on adaptation. Specifically, this part of the policy consists of communication of the current state of air quality, its associated health hazards, and the precautionary measures that the population should take. Local mass media (newspapers, radio, television) and official media (the AIRE CMDX app, official website, and social network accounts) are mandated by law to spread this information. Furthermore, once the alert (*contingencia*) is active, the CAMe performs constant evaluation of meteorological conditions and updates the population at 10 am, 3 pm, and 8 pm through the channels mentioned above.

[4] The evidence for China is mixed (Lin et al., 2011; Viard and Fu, 2015).

[5] Only pre-warnings, known as *precontingencias*, were issued, consisting solely of public health advisories. This category was eliminated in 2016.

[6] Alerts can also be triggered by PM, but only three PM alerts occurred during the observation period. These were regional alerts—a category not applicable for ozone—and covered different geographical areas. I exclude these episodes to avoid contaminating the control group.

Under normal conditions, Mexico City enforces the "Hoy No Circula" (HNC) program, which imposes license plate–based driving restrictions. This program prohibits 20% of the vehicles registered in the city from operating each weekday, on the basis of the last digit of their license plates.[7] Upon activation of a PCAA alert, the driving restrictions intensify significantly beyond the regular HNC schedule, affecting approximately half of the city's vehicles: Each alert alternates between restricting all vehicles with license plates ending in even digits and those with plates ending in odd digits.

Research indicates that Mexico City's standard HNC program does not effectively mitigate traffic congestion and may inadvertently worsen pollution over time, largely because the restrictions are fixed and predictable (Davis, 2008). However, the PCAA-induced restrictions differ from the regular HNC regime in two important ways: The selection of restricted cars varies by final license plate digit, and the restrictions are announced only one day in advance.

The policy seeks to achieve very short-run reductions in outdoor air pollutant concentrations. The PCAA mandates several industrial restrictions during an alert episode: a 40% reduction in emissions from all firms and factories with combustion processes or those that generate PM, a 50% operational reduction at the Jorge Luque and Valle de México thermoelectric plants, and the suspension of asphalt plants and combustion activities used for firing bricks, ceramics, and foundry in artisanal furnaces. These restrictions apply not only to all municipalities (*alcaldías*) within Mexico City but also to 18 neighboring municipalities in the State of Mexico, reflecting the transboundary nature of pollution and the regional coordination role played by the CAMe.

The Mexico City metropolitan area hosts a dense concentration of polluting facilities, many of them located near or within residential and commercial zones. According to RETC data, 82 out of the 170 industrial facilities within the area of study are located in the 18 participating municipalities of the State of Mexico, and these alone account for approximately 48.2% of total reported CO_2 emissions in the region.

An alert is activated when any monitoring station in the city surpasses the ozone concentration threshold. PCAA alerts are usually issued in the afternoon, when ozone reaches its maximum concentrations. The modal activation hour is 4 pm (32%), followed by 3 pm (24%) and 5 pm (24%). When the alert is announced, the government broadcasts health information and announces the measures to be taken. The industry restrictions take effect

[7] A vehicle emissions verification system assigns every city-registered vehicle to one of four categories (00, 0, 1, 2). Only vehicles in the 00 category are exempt from these restrictions.

immediately. The driving restrictions begin the next morning at 5 am.[8] Once the alert is active, a monitoring committee determines when pollution and weather conditions allow deactivation. Most alerts last between one and two days, with an average duration of 39 hours.[9]

3 Data

To estimate the impacts of Mexico City's air quality alert program, I utilize comprehensive, high-frequency data from a diverse range of sources. Specifically, my analysis incorporates data from seven areas: PCAA regulatory information and alerts, hospital-level health outcomes, monitor-level pollution and weather data, establishment-level annual emissions, sensor-level traffic data, administrative records from the subway and BRT systems, and daily citywide awareness data from Google Trends. This section details each of these data sources and provides descriptive statistics.

3.1 Pollution and weather data

I use monitor-level SIMAT data covering April 2016 to August 2019 for Mexico City. The network reports hourly average concentrations of PM_{10} ($\mu g\ m^{-3}$), ozone (ppb), NO_x (ppb), CO (ppm), and SO_2 (ppb). The sample includes 26 monitors for PM_10, 38 for ozone, 32 for NO_x, 33 for CO, and 35 for SO_2. SIMAT stations also measure weather variables, including wind speed and direction, relative humidity, and temperature, on the same hourly schedule. These meteorological indicators are incorporated as controls in all my RDD analyses. Monitor functioning suffers from a degree of intermittency. When an hourly reading for a monitor is missing, I impute the value using the inverse-distance-weighted average of the nearest three stations reporting that hour.[10] For regression analysis, the data are then aggregated to the hour–city level, yielding a balanced panel.

To examine spatial heterogeneity in pollution responses across monitors, I construct a treatment intensity measure based on each monitor's proximity to restricted industries. This measure combines the pollution data with facility-level emissions data for 2016 from the

[8] See Figure A.1, which focuses on the alert issued on August 7, 2016. This alert lasted 24 hours, so it was deactivated at 4 pm on August 8, 2016—the second red line in Figure A.1.

[9] Appendix Figure A.2 shows in detail the distribution of the alert duration: 26.7% last 24 hours or less, 53.3% last between 24 and 48 hours, and 20% last more than 48 hours.

[10] The imputation is conducted at the original hour–station level; it decreases the share of missing values from 21.7% to 0.2% for O_3, 29.4% to 0.6% for SO_2, 33.0% to 1.4% for CO, 41.6% to 4.9% for NO_x, and 52.2% to 15.1% for PM_{10}. Since the RDD analyses are conducted at the hour–city level, the final dataset has no missing values, as shown in Table A.3.

RETC, a self-reported inventory of annual emissions at establishment level, submitted by firms and enforced through oversight by the Federal Attorney for Environmental Protection (PROFEPA) under the Ministry of the Environment and Natural Resources (SEMARNAT). This registry is analogous to the Toxics Release Inventory in the US and the European Pollutant Release and Transfer Register (E-PRTR), as it follows the structure and reporting guidelines of the OECD PRTR framework (OECD, 2014; SEDEMA, 2018). It covers listed air and water pollutants and provides geographic coordinates for each reporting facility.

SO_2 is the pollutant most directly targeted by the industrial restrictions, but SO_2 emissions are not reported in the RETC. I therefore use each facility's reported CO_2 releases as a proxy for treatment intensity: Fossil-fuel combustion that generates SO_2 invariably produces CO_2, and CO_2 volumes scale with a plant's overall emissions potential. Section 6 describes how I aggregate this proxy to the monitor level to construct a proximity measure that accounts for both the number of nearby plants and the scale of each plant's emissions. This proxy correlates strongly with monitor-level SO_2 concentrations in the cross-section ($\rho > 70\%$), which provides empirical support for its use in the heterogeneity analysis.

3.2 PCAA documentation

The running variable (RV) of my main RDD specification—the difference between the citywide daily maximum ozone measurement and the alert threshold—is constructed from station-level pollution readings and the applicable pollution thresholds. The latter, along with the alert history, are derived from official communications published in the *Mexico City Gazettes*. I process the historical record of all alerts issued during the analyzed period and a detailed list of all the program's modifications since its inception to produce a daily variable indicating the applicable alert threshold, which remained constant during the period analyzed in this paper.[11]

Figure 1, Panel A, displays the daily maximum ozone readings during the analysis period alongside the alert activation threshold. The threshold is relatively high at 155 ppb, approximately 3.1 times the World Health Organization's (WHO's) guideline for daily ozone exposure (World Health Organization, 2021), meaning that only extreme pollution events trigger an alert under the PCAA program. In practice, just fifteen alerts were issued over the whole analysis period. This design feature is relevant for interpreting the results in light of the existing literature: A common concern about air quality warnings is that repeated or

[11]The program formally includes a Phase II, which entails additional industry and driving restrictions. However, no Phase II alerts have ever been issued, so this component is omitted from Table A.3 and from the rest of the analysis for simplicity.

long alerts may give rise to alert fatigue and reduced responsiveness (Saberian et al., 2017; Dangel and Goeschl, 2025). Panel B shows that the alerts were not only rare but also brief, with 80% lasting no more than 48 hours.

Figure 1: **PCAA alerts: Frequency and duration**

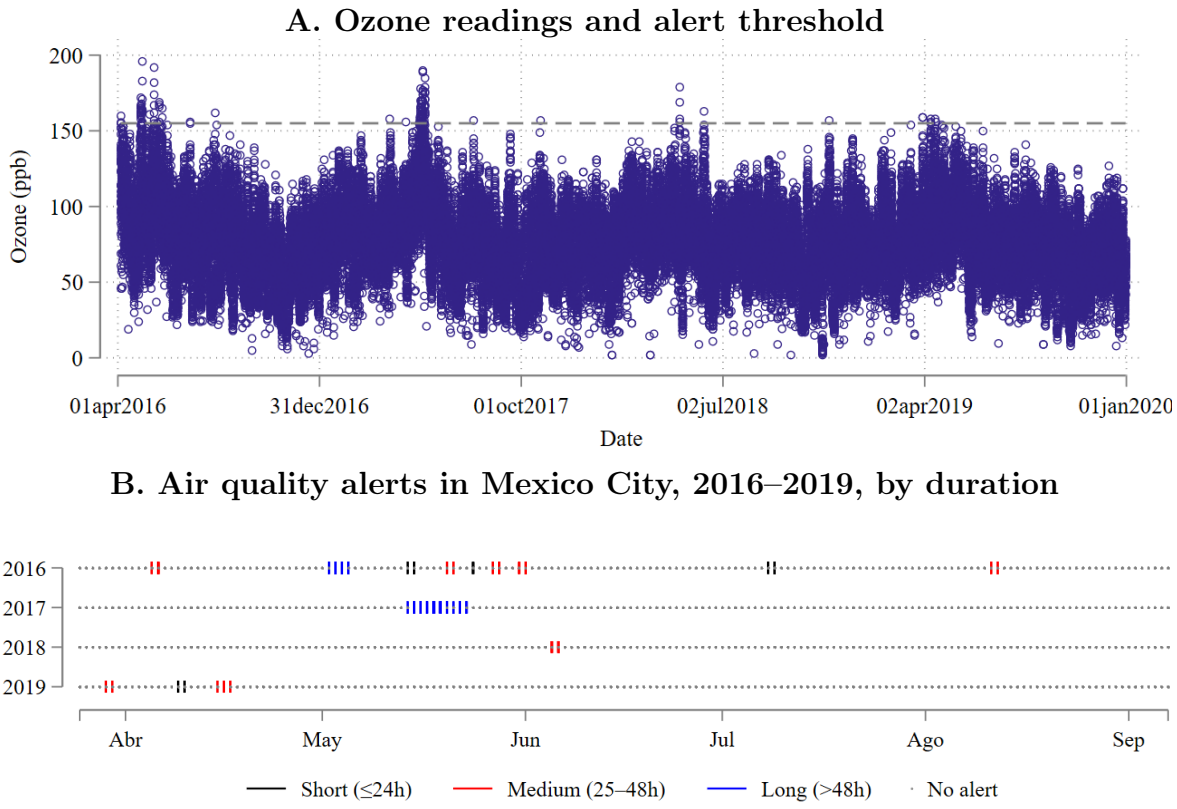

Note: Author's calculations from alert records and daily air quality readings. Panel (a) shows the maximum daily monitor-level ozone readings, measured in parts per billion, throughout the analysis period (01/04/2016–31/12/2019), with the dashed line representing the PCAA alert threshold. Panel (b) shows alert days, split by duration. Months without alerts throughout the sample are omitted from the visualization.

3.3 Urban flows

From the Mexico City Open Data Portal, I obtain hourly traffic data from 343 sensors and video detectors located throughout the city. This dataset encompasses over 10.3 million records, detailing hourly vehicular flow and average speeds from 2016 to 2019. Car counts are disaggregated by vehicle type. I use speed as a measure of overall congestion reductions caused by the alerts and leverage detailed car counts by vehicle type to scrutinize the workings of the policy. Appendix Figure A.3 shows the hourly average car count and speed, as

measured by the sensors and video detectors. The mirroring trends between these two variables show their complementary nature.

3.4 Health outcomes

To investigate the health impacts of PCAA alerts, I use data on ED visits for respiratory and cardiovascular diseases (CVDs), obtained from public hospital administrative records for Mexico's largest public healthcare system, which covers more than half of the population. These records are publicly available and include all hospitals under the Ministry of Health (Secretaría de Salud, SSA) system and national hospitals. There are 51 hospitals in the city in this subsystem, and they are well distributed across the city, as shown in Figure 2 discussed below. Until 2020,[12] the SSA hospitals provided care to individuals insured under Seguro Popular, the noncontributory healthcare system for informal or unemployed workers and the uninsured population. Recent estimates suggest that, in practice, the SSA network cares for over two-thirds of the population. Overall, while this sample lacks data from private hospitals, it does cover the bulk of the public health system. Only 7% of the population has private insurance nationwide, although there is considerable regional variation (Juan Lopez et al., 2015).

3.5 Awareness

Individuals might react to the alerts by avoiding exposure. A necessary condition for them to do so is that they have access to information about contemporaneous air quality and its health risks, whether directly through the alerts or by actively seeking additional information. To analyze the role of information-seeking behavior as a potential mechanism driving the health improvements caused by PCAA alerts, I propose an awareness measure using search indexes for relevant terms from Google Trends. By default, the Google Trends results are normalized by query time and location. These parameters are set for the years 2016–2019 and Mexico City, respectively. Each data point is divided by the total number of searches within the user-specified geography and time range to compare relative popularity. The resulting numbers are then scaled to a range of 0 to 100 based on a topic's search proportion within all searches.

I group search terms into four broad topics of interest: *pollution*, *symptoms*, *prevention*, and *PCAA*. Each category is designed to capture a distinct dimension of awareness, with

[12]Since 2020, the Mexican public healthcare system has been undergoing a transition toward universal coverage, leading to shifts in how care is organized between SSA establishments and other hospitals.

my goal being to distinguish information-seeking behavior aimed at complying with policy restrictions from behaviors explicitly aimed at improving the adoption of prevention measures or that reflect awareness of pollution-related symptoms. The *pollution* category focuses on general environmental conditions, including search terms such as "ozone" and "air quality." The *symptoms* category encompasses pollution-related health issues, with search terms such as "itchy eyes" and "cough." *Prevention* refers to protective actions or devices, including "face mask" and "air purifier," among others, and finally, *PCAA* encompasses terms directly linked specifically to the program, such as "contingency/contingencia" (the official name for the alert). The specific terms are grouped into each topic with the "+" operator in Google Trends, which functions as a logical OR. Hence, the output is a composite index of the relative popularity of each of these four topics over time within Mexico City. The set of terms for each topic, originally searched in Spanish, along with their corresponding English translations, is presented in Appendix Table A.2.

Appendix Figure A.4 shows the evolution of interest over time for the four constructed indices from April 2016 to December 2019. The *pollution* and *PCAA* topics display clear spikes during this period, whereas interest in *symptoms* and *prevention* fluctuates more irregularly and with no discernible pattern.

3.6 Descriptive statistics

Figure 2 shows the geographical distribution of the pollution monitors, hospitals, and traffic sensors collecting the data used in the analyses. The network includes 38 pollution monitors, 51 hospitals with EDs, and 343 traffic sensors. These are distributed throughout the Mexico City metropolitan area, with higher density in more populated and transit-intensive zones and sparse measurement in the rural and conservation areas in the south of the city.

Table A.3 provides descriptive statistics for the main variables employed. The table shows that the average hourly ozone levels in the city are 30.31 ppb. This average is high considering that the WHO's current guidelines recommend an 8-hour daily maximum of 60 $\mu g/m^3$ ($\sim$30 ppb) not to be exceeded more than 3–4 times per year WHO (2021). Similarly, average PM_{10} concentrations in the city are 42.53 $\mu g/m^3$, which far exceed the WHO annual guideline of 15 $\mu g/m^3$. This indicates significant health risks associated with ozone and PM pollution in Mexico City, consistent with the PCAA's use of the levels of these two pollutants as the criteria for its alerts.[13]

[13] As described in the empirical strategy section, I focus on alerts triggered by ozone given the rarity of PM_{10} alerts, which are excluded from the sample.

Figure 2: **Data: Sources and coverage**

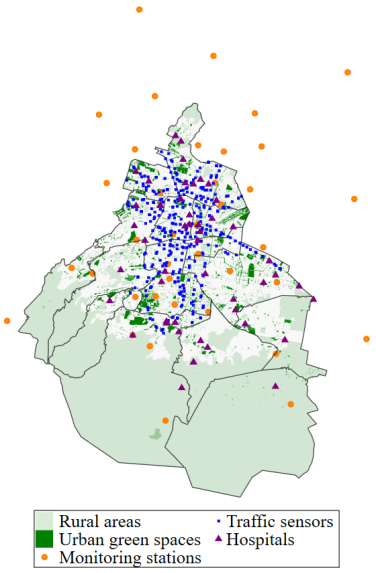

Note: The map displays the location of the data collection points for the main variables employed in this paper. These include a) weather and pollution monitoring stations, b) traffic monitors (sensors and video), and c) all public hospitals in Mexico City. Areas covered by vegetation, including urban green areas and rural zones, are highlighted in green.

For NO_x, the mean level is 39 ppb ($\approx$73 $\mu g/m^3$). While there are no specific guidelines for NO_x, these concentrations are well above the annual WHO guideline for NO_2 of 10 $\mu g/m^3$. In contrast, the average SO_2 concentration is 3.98 ppb ($\approx$ 10.5 $\mu g/m^3$), well below the WHO 24-hour guideline of 40 $\mu g/m^3$. Finally, the average CO level of 0.5 ppm ($\approx$ 0.57 $\mu g/m^3$) is also below the WHO 8-hour guideline of 4 $\mu g/m^3$, suggesting very low carbon monoxide pollution in the city.

Table A.3 also includes information on traffic, health, and public awareness. Panel (b) reports hourly traffic data, showing an average congestion speed of 47.37 km/h and vehicle counts dominated by cars (mean = 290,286.55), with smaller contributions from trucks, buses, and small buses/vans. Panel (c) summarizes hourly ED visits for respiratory and CVD diagnoses, with respiratory cases (mean = 11.58) being more frequent than CVD (mean = 3.14), for the general population and vulnerable age groups (under 5 and over 65 years old). Panel (d) shows the descriptive statistics for information-seeking behavior, employing the four measures proposed. Note that the levels cannot be compared across the measures since they are each adjusted with respect to their own distribution.

4 Empirical strategy

An alert is triggered whenever ozone levels surpass 155 ppb in any station in the city. Exploiting the arbitrariness of the PCAA alert threshold, I employ an RDD where the RV is the maximum ozone value relative to the threshold at t and the outcomes of interest are analyzed at $t+1$, when all restrictions are active. While the alert threshold is set by a Mexico City regulation, it is the Metropolitan Environmental Commission that receives the data and issues the alerts, such that there is an imperfect match between the air quality index and alerts. Hence, I employ a fuzzy regression discontinuity (FRD) methodology to identify the causal impacts of the PCAA. The FRD allows me to estimate the LATE of the program under specific assumptions (Hahn et al., 2001). The first assumption is monotonicity, which requires no local defiers whose behavior contradicts the treatment assignment rule. Given the centralized mode of alert activation, this assumption is reasonable.

The second assumption is that the instrument is relevant. Figure 3 evaluates treatment compliance by plotting the share of days with an alert along the RV, defined as the difference between the maximum ozone reading in the city and the 155 ppb threshold. Following Calonico et al. (2015), the number of evenly spaced bins is set to represent the overall variability of the raw data. I estimate the local linear fits separately on each side of the threshold using a triangular kernel and optimal bandwidth to minimize the mean squared error (MSE) of the resulting estimator, as in Calonico et al. (2017). Consistent with legislation, there is a discontinuous jump in the probability of a PCAA alert being issued, but the discontinuity is not sharp (i.e., 0 to 1), which supports my choice to use an FRD design. Quantitatively, I estimate that there is a 51.8-percentage-point greater likelihood of an alert's being triggered on days with peak hourly ozone readings just above the 155 ppb threshold than on days with readings just below it (Appendix Table A.4). The magnitude of this discontinuity implies that the LATE point estimates will be approximately 1.9 times larger than the ITT. The third assumption, local smoothness (Dong, 2018), implies that units cannot sort themselves around the threshold to attain or avoid treatment and is discussed in Section 4.1 below.

More formally, I derive estimates of the first stage, the ITT, and the LATE described above by estimating nonparametric local linear regressions of the following form:

$$Y_{it+1} = \beta_0 + \tau \text{Above}_t + f(\text{Daily Max Ozone}_t) + \varepsilon_{it}. \tag{1}$$

In Equation (1), Y_{it} is the dependent variable for hour i of day t. This variable represents one of the various outcomes of interest, such as daily hospital admissions, pollution levels,

or behavioral responses. Above_t is an indicator for whether a PCAA alert is triggered on day t based on the ozone rule. The term $f(\text{Daily Max Ozone}_t)$ serves as the RV in this RDD; it is a nonparametric function of the daily maximum ozone readings centered at the threshold (155 ppb). The term ε_{it} is a mean-zero idiosyncratic error term. For all outcomes, the parameter of interest is τ, the ITT.

In addition to presenting reduced-form results from Equation (1), I estimate LATEs using nonparametric local linear regressions of the following form:

$$Y_{it} = \beta_0 + \tau \text{Alert}_t + f(\text{Daily Max Ozone}_t) + \varepsilon_{it}. \tag{2}$$

Here, Alert_{it} is an indicator for whether hour i of day t was treated by a PCAA alert. Leveraging the RDD framework, I instrument for Alert_t with Above_t to obtain the LATE. Essentially, this rescaling adjusts the estimates from Equation (1) by the magnitude of the first-stage discontinuity.

As discussed, all the RDD specifications are estimated by means of nonparametric local linear regressions with a triangular kernel. This method, detailed in Calonico et al. (2019), consists of restricting the sample to observations near the threshold and estimating Equation (1) with a weighted least squares regression. To determine which observations are *near* the threshold, I use the h_{MSE} bandwidth selection algorithm, which determines which observations can be considered near the threshold by minimizing the asymptotic MSE of the RDD estimate given a kernel and polynomial order choice. I use a triangular kernel because it provides optimal weights for the h_{MSE} algorithm (Cattaneo et al., 2019) and employ linear polynomials ($p = 1$). I adjust the bandwidth selection algorithm and the inference of standard errors for a heteroskedasticity-robust nearest-neighbor variance estimator. The reported confidence intervals are constructed with robust bias correction as described in Calonico et al. (2014). In Section 7, I show that the interpretation of my findings is robust to variations in the polynomial order, kernel, and standard error choices. Finally, to adjust for weather patterns, I include hourly averages of weather conditions such as temperature, humidity, and wind speed.

4.1 RV manipulation

An important potential threat to the validity of my FRD design is that city officials could try to manipulate the RV to prevent the triggering of an alert. If the alerts inform the public about how bad air quality is, this could have political costs for incumbent administrators,

Figure 3: **Discontinuity in the probability of alert activation**

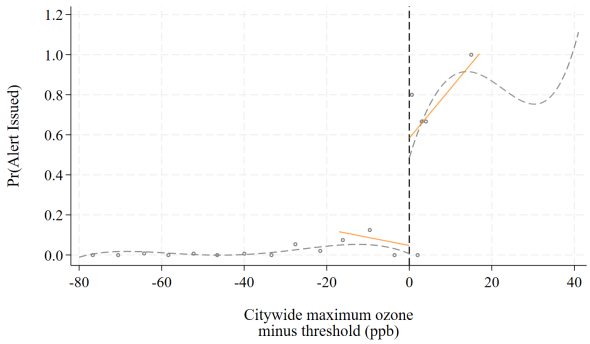

Note: The figure plots the discontinuity in the probability of an alert being activated around the ozone cutoff. The circles represent the local means of the outcome. Following Calonico et al. (2015), I compute these local means by partitioning the support of the RV into quantile-spaced bins. The number of bins is selected to represent the overall variability of the raw data. The solid lines depict local linear fits estimated separately on each side of the threshold with a triangular kernel, a local linear polynomial, and an optimal bandwidth h_{mse}, as in Calonico et al. (2017). The dashed lines are global fourth-order polynomials estimated separately on each side of the threshold.

as it has been found that exposure to information on poor air quality deteriorates trust in local government (Yao et al., 2022; Chen et al., 2024). However, manipulating reported pollution readings would be challenging because the data are publicly available and the alerts are issued in near real time, with an average lag of only three hours after the threshold is passed.

To investigate whether manipulation could have taken place, I test whether the RV's distribution is continuous at the threshold. In this context, if many more pollution readings fall just short of the threshold (to its left) than beyond it, this would suggest manipulation. Figure 4 employs the Cattaneo et al. (2019) and McCrary (2008) no-manipulation tests to rule out bunching around the alert threshold. Both figures confirm that the RV density is continuous around the threshold. The Cattaneo et al. (2019) test statistic confirms the visual test: Given the p-value of 0.992, I cannot reject the null hypothesis that the RV is continuous at the threshold.

Figure 4: **No-manipulation test**

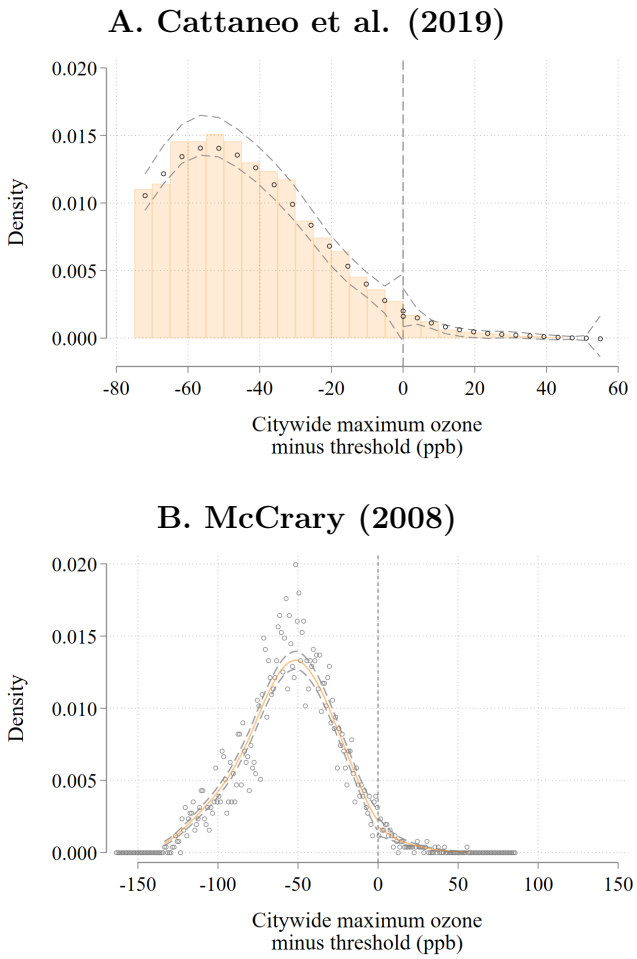

Note: Running variable is the daily city-level maximum pollution level relative to the alert threshold. Panel A employs the Cattaneo et al. (2019) test and Panel B the McCrary (2008) test.

5 Results

5.1 Impacts of PCAA alerts on air pollution

The PCAA program is a multipronged intervention designed to mitigate the health risks associated with extreme pollution episodes. Although data on the impacts of some policy components, such as real-time industrial production intensity by facility, are unavailable, the city's monitoring system provides rich pollution data and detailed inventories, enabling me to assess the program's effectiveness.

Automobile emissions are the leading source of emissions of CO and NO_x. Table 1 shows that transport accounts for more than 80% of CO emissions and more than 70% of NO_x (NO

and NO_2). On the other hand, area sources such as unpaved roads, urban waste, agriculture, vegetation, and construction drive the bulk of PM_{10} emissions, with only 12% attributable to personal cars and 22% to other vehicles. Automobile emissions are not a primary source of SO_2 in most contexts (Zhang et al., 2017), and Mexico City is no exception. Most SO_2 emissions in the city originate from industrial combustion processes, including in two large combined-cycle thermoelectric plants, chemical and metallurgic plants, and numerous asphalt and brick factories.

Table 1: **Emissions in Mexico City by particle and type of source**

	Total	**Industry**	**Area sources**	**Mobile sources**	**Others**
Particle			Emissions [ton/year]		
PM_{10}	35,274.0	3,574.3	20,015.3	10,899.1	785.3
$PM_{2.5}$	14,012.0	2,526.3	5,876.1	5,437.8	172.1
SO_2	2,466.0	1,150.8	980.7	334.0	0.0
CO	643,921.0	6,277.7	23,811.9	613,831.7	0.0
NO_x	140,156.0	11,915.0	14,264.1	112,350.0	1,627.2
		Industry	**Area sources**	**Mobile sources**	**Others**
Particle			Percentage		
PM_{10}		10.1%	56.7%	30.9%	2.2%
$PM_{2.5}$		18.0%	41.9%	38.8%	1.2%
SO_2		46.7%	39.8%	13.5%	0.0%
CO		1.0%	3.7%	95.3%	0.0%
NO_x		8.5%	10.2%	80.2%	1.2%

Note: Percentages calculated from the *Mexico City Emissions Inventory 2016*. This document, prepared by the Secretariat of the Environment, brings together the report of emissions of criteria pollutants, toxic gases and greenhouse effect compounds in 93 categories: 25 point sources, 55 categories of area sources, 11 types of vehicle sources and two natural sources. For the development of this inventory, methodologies described in the *Manuals of the Emissions Inventory Program of Mexico*, the California Environmental Protection Agency (CalEPA), the United States Environmental Protection Agency (US EPA) and the Intergovernmental Panel on Climate Change (IPCC) were used. Ozone is not included in the emissions inventories because it not directly emitted by any source but is formed when nitrogen oxides (NO_x) and volatile organic compounds (VOCs) react in the presence of sunlight.

Given this emissions composition, the effect of PCAA alerts on ozone levels hinges on their ability to influence the precursors of ozone formation and on the interactions between these changes. Ozone, a secondary pollutant, forms from NO_x and volatile organic compounds (VOCs) in the presence of sunlight through a process that depends on the concentrations of these precursors in nonmonotonic, nonlinear ways Zhang et al. (2017). This dependence can result in either NO_x-limited or VOC-limited regimes, affecting ozone formation rates

differently based on the availability of NO_x and VOCs.[14] In other words, the impact depends on both the effectiveness of the various restrictions imposed by the policy and the local chemical regime.

Figure 5: **Impact of PCAA alerts on next-day hourly O_3 levels**

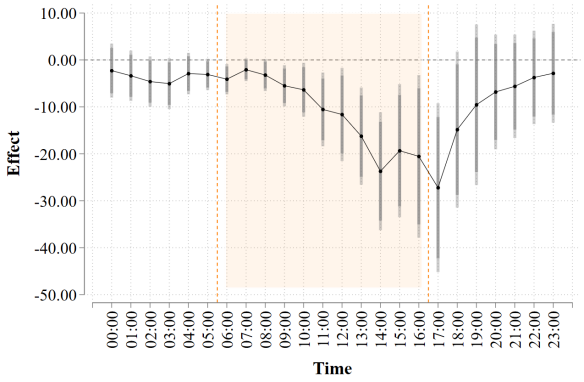

Note: The figure presents estimates of the intention-to-treat (ITT) effect for each hour of the day, derived with a triangular kernel, a local linear polynomial, and an optimal bandwidth h_{MSE}. All estimates are obtained with the `rdrobust` package by Calonico et al. (2017). The confidence intervals are computed with robust bias correction, following the approach of Cattaneo et al. (2019). All estimates include a vector of meteorological controls. The sample covers the period from April 4, 2016, to December 31, 2019. The figure shows 90% (dark gray) and 95% (light gray) confidence intervals.

Figure 5 demonstrates that alert activation significantly reduces ozone, the pollutant targeted by the policy levels, with the effect becoming more pronounced as the day progresses. Table 2, Column (a) shows that the average ITT effect on ozone throughout the day is substantial, with a reduction of 22.7 ppb, which amounts to nearly three-quarters of the sample mean of 31 ppb. The ITT captures the effect of ozone levels just above the regulatory cutoff, regardless of whether an alert is actually issued, and reflects real-world policy performance under imperfect implementation. The probability of an alert being triggered when the ozone threshold is exceeded in the pollution data increases by approximately 70%. With the aim of providing an estimate of the policy's potential under full enforcement, I scale up the LATE reported in Panel C considering this level of compliance.

The impacts of the PCAA alerts on daily average concentrations of other pollutants are also reported in Table 2. The results reveal a mixed pattern across pollutants but consistently large effects for those most closely tied to industrial activity. Reductions in SO_2

[14]In high-NO_x urban environments, increasing NO emissions can reduce ozone levels because of the NO_x titration effect, where NO reacts with ozone, converting it into NO_2 and oxygen (O_2). This effect is most pronounced in areas with high traffic or industrial activity and is especially relevant during the evening and night, when photochemical ozone formation slows. Conversely, in NO_x-limited environments, higher NO_x levels can increase ozone formation by generating oxygen radicals that drive ozone production.

are large: Alerts are associated with an average decrease of 4.5 ppb, equivalent to a 71% decline relative to the control mean (calculated from observations within the bandwidth but below the threshold). This finding suggests that the industrial restrictions activated by the alerts effectively curb SO_2 emissions. However, because SO_2 is not a precursor to ozone, these reductions are unlikely to explain the observed decrease in ozone concentrations.

Concentrations of NO_x and CO—both primarily emitted from vehicle combustion—show a more complex pattern. On average, both increase on alert days, indicating that the policy is not consistently successful in curbing transport-related emissions despite imposing strong restrictions on traffic. However, as discussed below, both pollutants also show reductions (noisy in the case of CO) during restricted afternoon hours, when ozone levels fall most sharply. The average increase in NO_x is not necessarily inconsistent with the ozone reduction, as higher NO_x can enhance ozone titration under NO_x-abundant (or VOC-limited) conditions (Lin, 2010). The increase in CO concentrations is of limited concern from a policy perspective: Baseline levels are already low, with a control mean of 0.42 ppm, which amounts to barely 5% of the WHO-recommended limit. In other words, Mexico City does not face a CO problem at the population level, and CO is not a meaningful target under the alert policy.

Table 3 disaggregates these effects by hour of day. For SO_2, the reductions persist across the day, consistent with the industrial restrictions remaining active. NO_x shows increases during the morning hours but declines between 1 pm and 5 pm, the same window during which ozone levels fall most steeply (see Figure 5). The CO results are mostly underpowered, with the changes throughout the day lacking statistical and economic significance.

Finally, PM_{10} concentrations also decline significantly during the afternoon hours. The temporal patterns for most of the particles suggest that the policy is more effective in reducing emissions during the afternoon, when most discretionary trips happen and thus there is more scope for reduction in the number of trips (Winick et al., 2008). For the case of PM_{10}, the reductions may reflect a combination of factors, including suppressed emissions from the limits on industry, power generation, construction, and waste burning and reduced resuspension of road dust due to lower vehicle traffic. The latter is particularly relevant in peripheral areas with unpaved or poorly maintained roads, where vehicle movement is a major source of PM. The evidence thus suggests an additional pathway through which traffic restrictions can improve air quality beyond tailpipe emissions.

Table 2: **Impact of PCAA alerts on pollution**

	O_3	SO_2	CO	NO_x	PM_{10}
	(1)	(2)	(3)	(4)	(5)
Panel A. First Stage	0.741	0.744	0.732	0.738	0.711
p-value	$p < 0.001$	$p < 0.001$	$p < 0.001$	$p < 0.001$	$p < 0.001$
CI 95%	[0.69;0.79]	[0.69;0.80]	[0.68;0.79]	[0.68;0.79]	[0.66;0.76]
Panel B. ITT	-22.688	-4.579	0.231	18.387	-3.599
p-value	$p < 0.001$	$p < 0.001$	$p < 0.001$	$p < 0.001$	0.230
CI 95%	[-26.732;-18.644]	[-6.209;-2.948]	[0.138;0.324]	[11.153;25.620]	[11.153;2.282]
Control Mean	31.429	6.351	0.422	33.739	52.415
Panel C. LATE	-30.628	-6.154	0.316	24.920	-5.060
p-value	$p < 0.001$	$p < 0.001$	$p < 0.001$	$p < 0.001$	0.233
CI 95%	[-36.690;-24.566]	[-8.431;-3.877]	[0.180;0.452]	[14.678;35.161]	[-13.372;3.251]
Bandwidth	4.9	4.9	5.1	5.0	5.4
Obs(left|right)	384|336	384|336	504|360	504|360	504|360

Note: Panels A and B present estimates of Equation (1) derived with a triangular kernel, a local linear polynomial, and an optimal bandwidth h_{MSE}. In Panel A, the dependent variable is a dummy variable indicating whether the alert is active. In Panel B, the control mean corresponds to the left-hand-side prediction of the nonparametric regression at the threshold. Panel C reports the local average treatment effect (LATE) calculated as the ratio of the intention-to-treat (ITT) effect to the first-stage estimate. All estimates are obtained with the `rdrobust` package by Calonico et al. (2017). The reported coefficients, p-values, and 95% confidence intervals are computed with robust bias correction, following the approach of Calonico et al. (2019). All estimates include a vector of meteorological controls.

Table 3: **Impact of PCAA alerts on pollution, by time of the day**

	SO_2				CO			
	00 to 05	**06 to 12**	**13 to 17**	18 to 23	00 to 05	**06 to 12**	**13 to 17**	18 to 23
	(1)	(2)	(3)	(4)	(5)	(6)	(7)	(8)
Panel A. First Stage	0.577	0.674	0.529	0.555	0.587	0.670	0.562	0.544
p-value	$p < 0.001$	$p < 0.001$	$p < 0.001$	$p < 0.001$	$p < 0.001$	$p < 0.001$	$p < 0.001$	$p < 0.001$
CI 95%	[0.46;0.70]	[0.57;0.78]	[0.42;0.63]	[0.46;0.65]	[0.46;0.71]	[0.57;0.77]	[0.46;0.67]	[0.44;0.65]
Panel B. ITT	-5.296	-7.011	-1.656	-0.314	0.166	0.302	-0.001	0.025
p-value	$p < 0.001$	$p < 0.001$	$p < 0.001$	0.537	$p < 0.001$	$p < 0.001$	0.953	0.503
CI 95%	[-7.787;-2.805]	[-9.395;-4.626]	[-2.545;-0.767]	[-1.311;0.683]	[0.078;0.253]	[0.139;0.464]	[-0.047;0.045]	[0.097;-0.047]
Control Mean	6.410	9.357	4.014	2.215	0.234	0.410	0.557	0.479
Panel C. LATE	-9.178	-10.400	-3.037	-0.564	0.283	0.451	-0.002	0.045
p-value	$p < 0.001$	$p < 0.001$	$p < 0.001$	0.530	0.002	0.002	0.954	0.508
CI 95%	[-13.997;-4.358]	[-14.352;-6.448]	[-4.632;-1.441]	[-2.322;1.195]	[0.103;0.463]	[0.170;0.731]	[-0.083;0.078]	[0.180;-0.089]
Bandwidth	8.2	6.3	20.5	11.2	8.2	6.7	19.3	8.9
Obs(left|right)	204|108	189|112	520|125	288|120	204|108	189|112	490|125	204|108
	NO_x				PM_{10}			
	00 to 05	**06 to 12**	**13 to 17**	18 to 23	00 to 05	**06 to 12**	**13 to 17**	18 to 23
	(1)	(2)	(3)	(4)	(5)	(6)	(7)	(8)
Panel A. First Stage	0.599	0.660	0.536	0.572	0.606	0.683	0.540	0.553
p-value	$p < 0.001$	$p < 0.001$	$p < 0.001$	$p < 0.001$	$p < 0.001$	$p < 0.001$	$p < 0.001$	$p < 0.001$
CI 95%	[0.48;0.72]	[0.56;0.76]	[0.43;0.64]	[0.47;0.68]	[0.48;0.73]	[0.58;0.79]	[0.44;0.65]	[0.45;0.66]
Panel B. ITT	9.759	26.028	-1.627	-1.934	-1.690	-0.394	-16.760	-14.910
p-value	$p < 0.001$	$p < 0.001$	0.050	0.326	0.608	0.935	$p < 0.001$	0.006
CI 95%	[4.684;14.835]	[14.843;37.212]	[-3.253;-0.001]	[-5.796;1.929]	[-8.148;4.768]	[-9.813;9.024]	[-22.816;-10.704]	[-25.541;-4.280]
Control Mean	19.013	33.603	29.551	33.154	44.067	53.622	51.633	50.978
Panel C. LATE	16.308	39.424	-2.937	-3.380	-2.780	-0.578	-30.299	-26.950
p-value	0.001	$p < 0.001$	0.035	0.316	0.606	0.935	$p < 0.001$	0.010
CI 95%	[6.795;25.821]	[19.510;59.337]	[-5.672;-0.201]	[-9.981;3.222]	[-13.339;7.778]	[-14.512;13.355]	[-40.590;-20.008]	[-47.370;-6.530]
Bandwidth	7.5	7.2	18.6	7.5	7.0	6.0	17.5	8.4
Obs(left|right)	180|102	210|119	455|125	180|102	180|102	189|112	390|125	204|108

Note: Panels A and B present estimates of Equation (1) derived with a triangular kernel, a local linear polynomial, and an optimal bandwidth h_{MSE}. In Panel A, the dependent variable is a dummy variable indicating whether the alert is active. In Panel B, the control mean corresponds to the left-hand-side prediction of the nonparametric regression at the threshold. Panel C reports the local average treatment effect (LATE) calculated as the ratio of the intention-to-treat (ITT) effect to the first-stage estimate. All estimates are obtained with the `rdrobust` package by Calonico et al. (2017). The reported coefficients, *p*-values, and 95% confidence intervals are computed with robust bias correction, following the approach of Calonico et al. (2019). All estimates include a vector of meteorological controls.

5.2 Impacts of air quality warnings on health

Ultimately, the central question is whether the PCAA alerts translate into better health outcomes. As discussed above, the program is designed primarily as a public health intervention rather than as a long-term pollution abatement measure. Table 4 summarizes the effects of alerts on ED visits for respiratory and CVD diagnoses across all ages and for vulnerable groups (children younger than 5 and adults older than 65). The first-stage estimates again show strong compliance, with a significant jump in alert activation across all specifications.

The ITT and LATE estimates point to substantial reductions in respiratory morbidity following an alert. The average hospital records 4.9 fewer respiratory ED visits per day for the general population (LATE, $p = 0.008$), a 56% drop relative to the control mean of 8.76. For vulnerable groups, the estimated reduction is 2.1 daily visits (LATE), or approximately 50% of the baseline average of 4.14. These are sizable effects, especially considering that respiratory ED visits are one of the key outcomes the alert system aims to prevent. For CVD cases, the estimated effects are smaller and less precise. The LATE estimate for the general population corresponds to a reduction of 1.2 visits per hospital per day—roughly a 45% drop from the control mean of 2.68—but is only marginally significant. Among vulnerable patients, the estimated decline is smaller in both absolute and relative terms and not statistically significant.

These findings indicate that improvements in air quality, specifically reductions in harmful pollutants such as ozone, SO_2, and PM,[15] likely reduce the incidence of severe respiratory episodes, despite the short-lived increase in NO_x and CO. The similar relative magnitudes of the effects among the general population and vulnerable groups suggest that it is unlikely that the health effects are entirely driven by the information component of the policy. If the effects operated entirely through an avoidance channel, we would expect to see greater impacts on vulnerable populations since the messaging targets them. This ordering of effects is also consistent with previous findings showing that acute pollution shocks have more immediate impacts on respiratory than on cardiovascular conditions (Brink et al., 2019; Schlenker and Walker, 2016). As a placebo check, Section 7 shows no significant effects of the alerts on outcomes unrelated to acute pollution exposure, such as cancer and digestive diseases.

Benchmarking the absolute magnitude of these effects against the effect sizes in the existing literature is challenging because many studies focus on isolating the impact of reductions

[15]The PCAA targets ozone and PM as the key pollutants that trigger alerts, given the severe health risks that they pose. The WHO also recognizes both as primary air pollutants affecting human health (World Health Organization, 2024).

in a single pollutant while holding information provision constant. In contrast, the context here features simultaneous responses from multiple pollutants, and the policy is highly salient to the public. By way of comparison, Fan et al. (2023) estimate that a 1 μg/m^3 reduction in SO_2 concentrations leads to a 0.9% decrease in cardiovascular deaths among people over 60 years and a 1.5% decrease among children under 5. Extrapolation of these results to a 7 ppb (18 μg/m^3) decrease would imply a reduction of ≈20% in ED visits among vulnerable populations. This figure is substantially lower than my ITT estimate, which reflects a 40% reduction for the same age groups. However, Neidell (2009) highlights the significant impact of information provision itself, finding that controlling for information increases the estimated effect of ozone by approximately 160% for children and 40% for elderly people. Accounting for this scaling effect would make my estimate more comparable, though direct comparisons remain difficult because of the simultaneous responses of multiple pollutants.

Table 4: **Impact of PCAA alerts on ED visits**

	Respiratory (All)	Respiratory (<5 and >65)	CVD (All)	CVD (<5 and >65)
	(1)	(2)	(3)	(4)
Panel A. First Stage	0.739	0.739	0.738	0.733
p-value	$p < 0.001$	$p < 0.001$	$p < 0.001$	$p < 0.001$
CI 95 percent	[0.69;0.79]	[0.69;0.79]	[0.69;0.79]	[0.68;0.79]
Panel B. ITT	-3.607	-1.539	-0.869	-0.357
p-value	0.007	0.039	0.067	0.093
CI 95 percent	[-6.24;-0.98]	[-3.00;-0.08]	[-1.80;0.06]	[-0.77;0.06]
Control Mean	8.756	4.140	2.684	1.012
Panel C. LATE	-4.882	-2.082	-1.178	-0.487
p-value	0.008	0.042	0.070	0.097
CI 95 percent	[-8.51;-1.25]	[-4.09;-0.08]	[-2.45;0.10]	[-1.06;0.09]
Bandwidth	5.0	5.0	5.0	5.1
Obs(left|right)	384|336	384|336	384|336	504|360

Note: All estimates include a vector of covariates **X**, which incorporates contemporaneous weather variables. Panels A and B present estimates of Equation (1) derived with a triangular kernel, a local linear polynomial, and an optimal bandwidth h_{MSE}. In Panel A, the dependent variable is a dummy variable indicating whether the alert is active. In Panel B, the control mean corresponds to the left-hand-side prediction of the nonparametric regression at the threshold. Panel C reports the local average treatment effect (LATE) calculated as the ratio of the intention-to-treat (ITT) effect to the first-stage estimate. All estimates are obtained with the `rdrobust` package by Calonico et al. (2017). The reported coefficients, p-values, and 95% confidence intervals are computed with robust bias correction, following the approach of Calonico et al. (2019).

6 Mechanisms

The health impacts discussed above likely reflect the combined operation of two key mechanisms. Clearly, improvements in air quality are consistent with a mitigation pathway. The previous section documented sharp reductions in criteria pollutants, suggesting that the restrictions on industrial activity and vehicle use effectively reduce emissions. Second, the policy's health messaging may prompt behavioral adaptation, such as staying indoors or reducing physical activity, which can lower individual exposure to pollution. In this section, I provide more direct evidence to test these two pathways: I investigate the adaptation channel using patterns of information-seeking behavior and characterize the mitigation channel by analyzing changes in industrial activity and vehicle usage.

6.1 Adaptation

One mechanism for the health results could be that individuals react by avoiding exposure to pollution when they become aware of an air quality warning. To investigate this conjecture, I explore whether individuals respond to the policy announcement with information-seeking behavior that might support their self-protection measures. Specifically, I use the search indexes for the four topics detailed in Section 3.5, designed to capture information-seeking corresponding to different behavioral responses: a) air quality levels, b) exposure symptoms, c) prevention/avoidance measures and d) the PCAA program restrictions.

Figure 6 plots the evolution of interest over time in these four topics in a 10-day window around an alert. The figure displays the coefficients for the time relative to alert activation, adjusted for seasonality and conditional on the inclusion of day-of-the-year and day-of-the-week fixed effects. The omitted category includes all days outside this window. I restrict the length of the window to five days before and after an alert is issued to avoid overlap in the windows of analysis. Time $j = 0$ indicates the date when the alert is issued, and time $j = 1$ is the date when the driving restrictions become active.

The results provide suggestive evidence that individuals' responses are more geared toward understanding air quality (Panel A) and especially the policy itself (Panel D), potentially indicating that their search is aimed at ensuring compliance with driving restrictions. When I look specifically at searches for pollution-related symptoms (Panel B) and searches that might support adaptation behaviors (Panel D), the trends for alert days are not statistically different from those for nonalert days.

Figure 6: **Impacts of PCAA alerts on pollution interest/awareness**

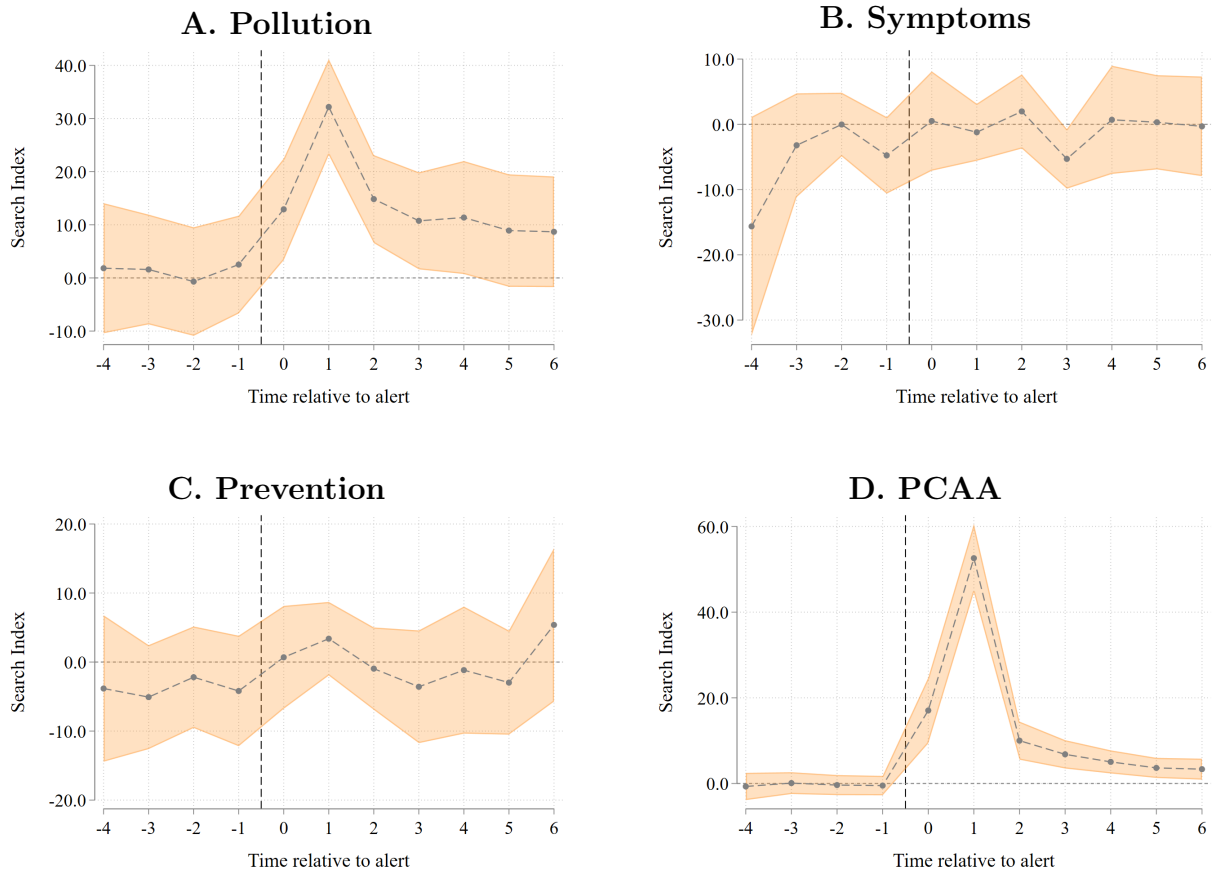

Note: Figures A to D show the normalized Google Trends search index for four topics: *pollution*, *symptoms*, *prevention*, and *PCAA*. The topic *pollution* includes the following combined Spanish search terms: "*contaminación*," "*smog*," "*ozono*," "*IMECA*," "*calidad del aire*," "*aire libre*," and "*contaminación ambiental*." *Symptoms* includes "*asma*," "*alergia*," "*dificultad para respirar*," "*ojos irritados*," and "*problemas respiratorios*." *Prevention* includes "*prevención*," "*exposición al aire*," "*mascarilla*," "*filtro*," "*purificador de aire*," and "*cubrebocas*." *PCAA* (Programa para Contingencias Ambientales Atmosféricas) includes "*contingencia ambiental*," "*alerta ambiental*," "*fase 1*," "*fase 2*," "*semáforo ambiental*," and "*programa PCAA*." Data span from 2016 to 2019 and are restricted to Mexico City. Search results are normalized by query time and location. All models include fixed effects for year, month, and day of the week.

Next, I apply an RDD approach using the four search indexes, but the analysis is constrained by lower statistical power because I have fewer observations and the spatial resolution of the outcomes is coarser. Appendix Table A.6 presents mixed, statistically insignificant effects. Except for air pollution searches, for which the estimates are extremely noisy ($p = 0.95$), the coefficient signs are consonant with theory: The changes in searches about protective behaviors, prevention, and the PCAA program are positive ($p = 0.14$ and $p = 0.33$), suggesting spikes in information-seeking. Meanwhile, searches for certain symptoms decline ($p = 0.16$), consistent with the health improvements documented in Section

5.2.

6.2 Mitigation

6.2.1 Impacts of PCAA alerts on mobility patterns

Prior research on Mexico City's permanent driving restriction program Hoy No Circula shows that it led many drivers to purchase an older, more polluting second vehicle, which undermined its environmental goals (Davis, 2008). While PCAA alerts are plausibly exogenous, preventing drivers from purchasing vehicles in anticipation of specific alerts, many residents may still respond by using a backup vehicle on alert days. Accordingly, what sign we should expect for the policy's effect on vehicle emissions is unclear.

Evidence on changes in vehicle usage is presented in Table 5. Both the ITT and LATE estimates indicate compliance with the restrictions of over one-half. Full compliance would mean that roughly half the cars are removed from the streets, which would amount to a reduction of approximately 142,000 vehicles per hour. The ITT estimate shows a decline of 77,206 cars, while the LATE estimate reaches 105,000. Notably, the LATE confidence interval does not allow me to rule out full compliance. The magnitude of the reductions is similar for larger vehicles such as trucks and buses.

These traffic reductions translate into measurable improvements in congestion, captured by increases in citywide average speeds. On alert days, average speed rises by approximately 2 km/h, representing a 4% increase over the control mean. While seemingly modest, this change is comparable in magnitude to the impacts of high-profile programs such as congestion pricing in New York City (Cook et al., 2025).[16]

[16] Appendix Table A.5, which disaggregates the effects over time, suggests that the policy may have become more effective in more recent years. In the first third of the sample period, alerts significantly reduced heavy vehicle counts but had no detectable effect on cars or congestion. For the final third of the period, significant reductions appear across all vehicle types and in average traffic speed. Additionally, in the most recent subsample, there is perfect compliance in the first stage, allowing a sharp RDD to be employed. Given that there are only 15 alerts in total during the analyzed period, these comparisons are limited by sample size.

Table 5: **Impact of PCAA alerts on hourly vehicle trips**

	Congestion (average speed)	Cars	Trucks	Buses	Small buses/vans
		(hourly vehicle trips)			
	(1)	(2)	(3)	(4)	(5)
Panel A. First Stage	0.736	0.733	0.631	0.642	0.655
p-value	$p < 0.001$	$p < 0.001$	$p < 0.001$	$p < 0.001$	$p < 0.001$
CI 95 percent	[0.68;0.79]	[0.68;0.79]	[0.58;0.68]	[0.59;0.69]	[0.60;0.71]
Panel B. ITT	1.57	-77,206	-6,238	-8,685	-29,032
p-value	0.011	$p < 0.001$	0.019	0.004	0.003
CI 95 percent	[0.36;2.79]	[-113,517;-40,896]	[-11,432;-1,044]	[-14,575;-2,795]	[-48,208;-9,855]
Control Mean	48.5	284,515	26,399	33,109	114,790
Panel C. LATE	2.14	-105,349	-9,882	-13,517	-44,293
p-value	0.011	$p < 0.001$	0.018	0.004	0.003
CI 95 percent	[0.493;3.79]	[-155,703;-54,995]	[-18,052;-1,711]	[-22,625;-4,409]	[-73,303;-15,284]
Bandwidth	5.0	5.1	8.2	7.5	6.8
Obs(left|right)	504|360	504|360	816|432	720|408	648|384

Note: All estimates include a vector of covariates $\mathbf{X}$, which incorporates contemporaneous weather variables. Panels A and B present estimates of Equation (1) derived with a triangular kernel, a local linear polynomial, and an optimal bandwidth h_{MSE}. In Panel A, the dependent variable is a dummy variable indicating whether the alert is active. In Panel B, the control mean corresponds to the left-hand-side prediction of the nonparametric regression at the threshold. Panel C reports the local average treatment effect (LATE) calculated as the ratio of the intention-to-treat (ITT) effect to the first-stage estimate. All estimates are obtained with the `rdrobust` package by Calonico et al. (2017). The reported coefficients, *p*-values, and 95% confidence intervals are computed with robust bias correction, following the approach of Calonico et al. (2019).

An interesting result from Table 5 is that, although the policy restricts car usage, this is not offset by an increase in public transport supply. Columns (4) and (5) show that the number of buses and small buses (known as *peseros*)—which are key modes of public transport in terms of volume of daily passengers, especially in the periphery—also decrease. This may reflect the fact that many of these vehicles have remained highly polluting until very recently (SEMOVI, 2019; Redacción Obras, 2025).

Table 6 examines the effect of the air quality warnings on public transportation usage. I find no significant changes in subway, BRT (Metrobus), or public bicycle usage, although the FRD estimates are negative for these three variables. Even on regular days, the public transportation system is overcrowded (SEMOVI, 2019) and uncomfortable (INFOCDMX, 2023). Hence, if an expansion in supply does not accompany the driving restrictions, those who can will choose to use private alternatives (including second cars but also taxis and rideshare services) instead of contributing to a stronger reduction in private trips.[17] The

[17]According to a public opinion survey conducted in Mexico City in 2010 with 2,500 participants, most

lack of increase in the use of these alternative modes of transport might also be linked to the public health messaging activated as part of the alerts: People are advised to avoid outdoor activities such as walking, which complements public transport usage.

Table 6: **ITT effect on public transportation**

	Metro	Metrobus	Ecobike
	(1)	(2)	(3)
Panel A. ITT	-16,841.904	-250,273.391	-3,029.042
p-value	0.611	0.168	0.609
CI 95%	[-81,772.758 ; 48,088.95]	[-605,845.789 ; 105,299.008]	[-14,639.424 ; 8,581.34]
Control Mean	368,998	1,033,175	18,225
Bandwidth	16.36	12.43	13.26
Obs(left|right)	852 | 288	51 | 20	55 | 21

Note: Panel A presents the intention-to-treat (ITT) estimates derived with a triangular kernel, a local linear polynomial, and an optimal bandwidth h_{MSE}. The control mean corresponds to the left-hand-side prediction of the nonparametric regression at the threshold. All estimates are obtained with the `rdrobust` package by Calonico et al. (2017). The reported coefficients, p-values, and 95% confidence intervals are computed with robust bias correction, following the approach of Calonico et al. (2019). All estimates include a vector of meteorological controls.

6.2.2 Impacts of PCAA alerts on industrial emissions

If reductions in industrial emissions drive the air quality improvements, then the treatment effects should be larger at monitoring stations located near the industrial establishments most affected by alert-driven restrictions. To explore this hypothesis, I match the locations of air quality monitors with nearby industries listed in the city's 2016 RETC inventory, which reports annual industrial emissions by pollutant according to OECD PRTR guidelines (OECD, 2014). Using each establishment's North American Industry Classification System (NAICS) industry code, I classify industries as either restricted or unrestricted, depending on whether their activities are subject to operational limits under the alert guidelines (GDF, 2016). Figure 7 shows the geographical distribution of restricted and unrestricted facilities within Mexico City and the 18 neighboring municipalities covered by PCAA directives. Restricted facilities are required to reduce emissions under the PCAA program, whereas unrestricted facilities can continue operating during alerts. The figure indicates that the majority of reporting industries in the area are subject to PCAA operational constraints. Appendix Table A.7 lists the restricted industries and their corresponding subsectors.

respondents described public transportation as uncomfortable (67%) and unsafe (61%). Only 21% considered it affordable, and just 14% described it as "fast" (El Poder del Consumidor, 2010).

Although the RETC does not report SO_2 releases, it does include CO_2, which I propose as a proxy for establishment-specific emissions intensity. This choice is motivated by the fact that fossil fuel combustion processes that emit SO_2 invariably generate CO_2 so facilities with higher CO_2 releases generally have higher fuel throughput and energy use. Emission inventories have documented that many stationary sources, including power plants, release both CO_2 and SO_2, although the exact emission ratios vary by fuel type, combustion technology, and pollution control measure (Smith et al., 2011; Guevara et al., 2024). Likewise, cross-sector studies document a robust positive correlation between CO_2 emissions, industrial energy consumption, and total output (Li et al., 2023a).

CO_2 emission intensity is expressed as the standardized density of estimated emissions (tons per year), calculated as the sum of emissions from all facilities subject to PCAA restrictions within a specified radius from a pollution monitor. Variation in monitor-level estimated emissions intensity can come from two margins: It can increase in the presence of a larger number of restricted establishments in the vicinity or from higher intensity per facility. The premise is that monitors located in areas with higher emissions intensity would experience larger air quality improvements during a PCAA alert.

Figure 7: **Location of Monitoring Stations and Industrial Facilities by Restriction Status**

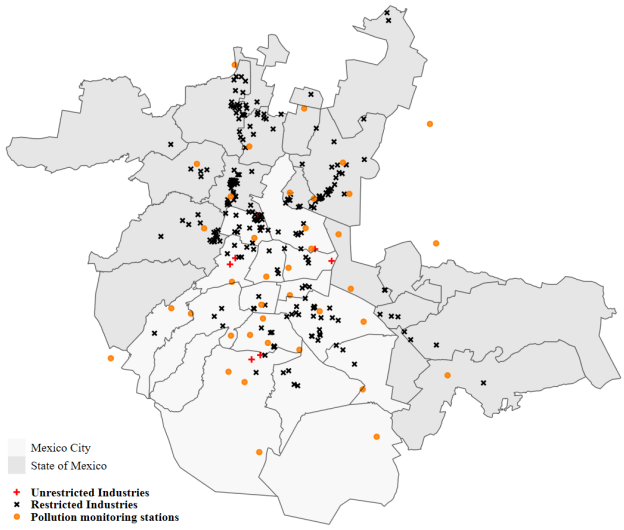

Note: This map displays the location of air quality monitoring stations (orange dots) and industrial facilities subject to restrictions during environmental alerts in Mexico City and the neighboring municipalities in the State of Mexico. Facilities included in the 2016 RETC (Registro de Emisiones y Transferencia de Contaminantes) are classified based on their North American Industry Classification System (NAICS) code into restricted industries (black $\times$) and unrestricted ones (red $+$).

As a first step, I assess whether CO_2 emissions intensity can serve as a credible proxy

for SO_2 exposure across varying distances from the monitors. Figure 8, Panel A, shows that for 15 km, 20 km, and 25 km radii, annual average emissions intensity correlates well with monitor-level SO_2 concentrations, suggesting that the proposed measure is a valid proxy for industrial SO_2 exposure.[18] The correlation peaks at the 15 km radius, reaching 77%, followed by 20 and 25 km with approximately 72%. A smaller buffer (10 km) performs worse, potentially because particle transport occurs over longer distances and because, under this radius size, four of the 38 restricted establishments are excluded ($n = 34/38$), which may introduce noise.

For each station and radius, I calculate and use the CO_2 emission intensity from restricted plants to estimate the effects separately for low- and high-intensity exposure groups, defined as the bottom and top terciles of the distribution shown in Panel A. Panel B of Figure 8 presents RD estimates of the effect of air quality alerts on hourly average SO_2 concentrations at monitoring stations derived with this heterogeneity measure. The results indicate that monitors exposed to higher industrial emissions experience larger reductions in SO_2 than those exposed to lower emissions intensity. This pattern holds across all radii except 10 km, which shows the weakest correlation with SO_2 concentrations. For 15 km, the point estimate for sensors exposed to high-intensity emissions is -7.83, more than twice that for low-intensity areas (-3.78), and the difference is statistically significant ($p = 0.02$).[19] For the 20 km radius, the estimated coefficient for high-intensity areas is -6.76, compared to -3.57 for low-intensity areas ($p = 0.05$), and for the 25 km radius, the estimates are -6.39 and -3.68, respectively ($p = 0.08$).

These findings are consistent with the industrial restrictions accounting for the geographical heterogeneity in SO_2 improvements and corroborate the conclusion that the policy is highly effective in curbing industrial emissions. Appendix Table A.7 lists all restricted industries, sorted by aggregate yearly CO_2 emissions. The table shows that the sectors driving the results—based on their contribution to annual industrial emissions—are the chemical industry, electric power generation, cellulose and paper, wood products, and metallurgy, with the top ten emitting NAICS industries concentrated within these sectors.

[18] In this main exercise, I construct the proxy intensity considering only establishments from restricted industries, which account for the majority of facilities in the city. Appendix Figure A.5 A shows the results from the same exercise considering all industries in the Mexico City area.

[19] We can reject the hypothesis that $\beta_{high} = -3.78$ at standard significance levels ($p = 0.02$).

Figure 8: **Heterogeneity by treatment intensity**

A. Monitor-Level SO_2 and Nearby Industrial Pollution – PCAA Sample

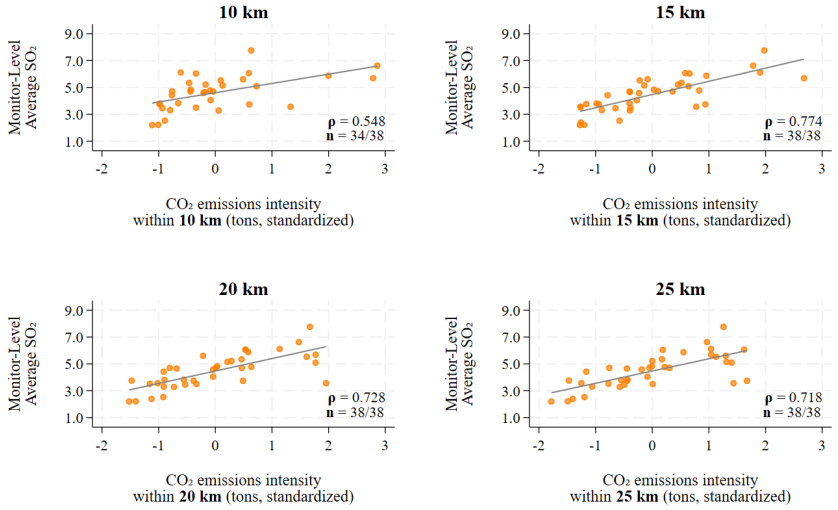

B. RD Estimates by Industrial Emissions Intensity

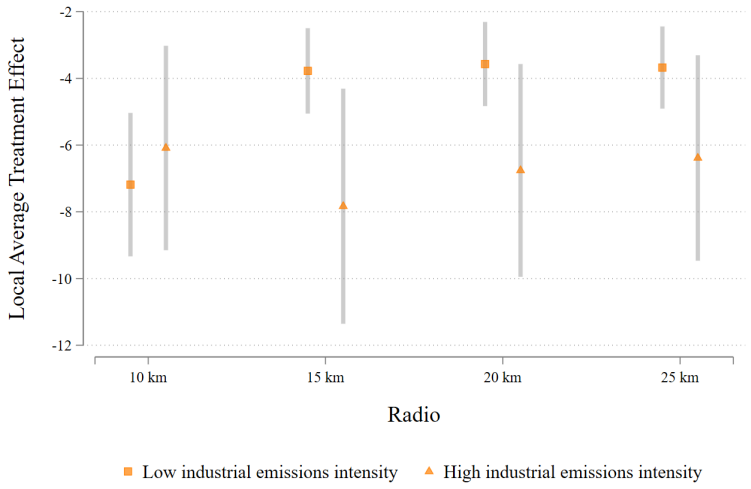

Note: Each scatterplot in Panel A shows the correlation between the average SO_2 concentration recorded at each monitoring station (y-axis) and the intensity of nearby industrial CO_2 emissions within 10, 15, 20, and 25 km (x-axis). The value of ρ denotes the Pearson correlation coefficient. The value of n indicates the number of monitoring stations with at least one restricted facility located within the corresponding radius. A linear fit is included to guide interpretation. In Panel B, the plotted coefficients correspond to local average treatment effects (LATEs) estimated via a fuzzy regression discontinuity design using the ozone threshold rule, based on Equation (1). Vertical bars show 95% confidence intervals.

7 Robustness checks

Given that estimating the RDD results requires a choice of bandwidth selection algorithm, local polynomial degree, and kernel, I next show that the main results are not sensitive to the choice of these tuning parameters. In particular, I focus on the key result of the PCAA alerts' impact on respiratory ED visits.

Figure 9 examines the robustness of the LATE estimates for respiratory-related ED visits under various specifications. Panel A explores how the LATE estimates vary by bandwidth selection algorithm, comparing the MSE-optimal, coverage error rate (CER-) optimal, and other alternatives. Panel B evaluates the sensitivity of the estimates to changes in the degree of the local polynomial used, with a range from linear (P1) to cubic (P3). Panel C investigates sensitivity to different kernel types, including triangular, Epanechnikov, and uniform kernels. Across all the panels, the results remain consistent, with the confidence intervals of the baseline specification (first estimate in each panel) including the estimates derived under these different methodological choices.

If pollution records were manipulated to prevent a PCAA alert, the observations closest to the threshold would be the likeliest to be manipulated. I thus include a donut hole regression, which tests the sensitivity to the exclusion of the observations within 2 and 4 ppb of the threshold (1 ppb and 2 ppb radius, respectively). The results are shown in Figure 9, Panel D. As shown in Figure 4, the alert threshold is quite lax, such that the percentage of observations falling above it is small. This limitation makes the results from the donut hole test rather noisy, but the figure shows that the estimates obtained are comparable to the baseline estimates.

Figure 9: **Robustness of LATE estimates**

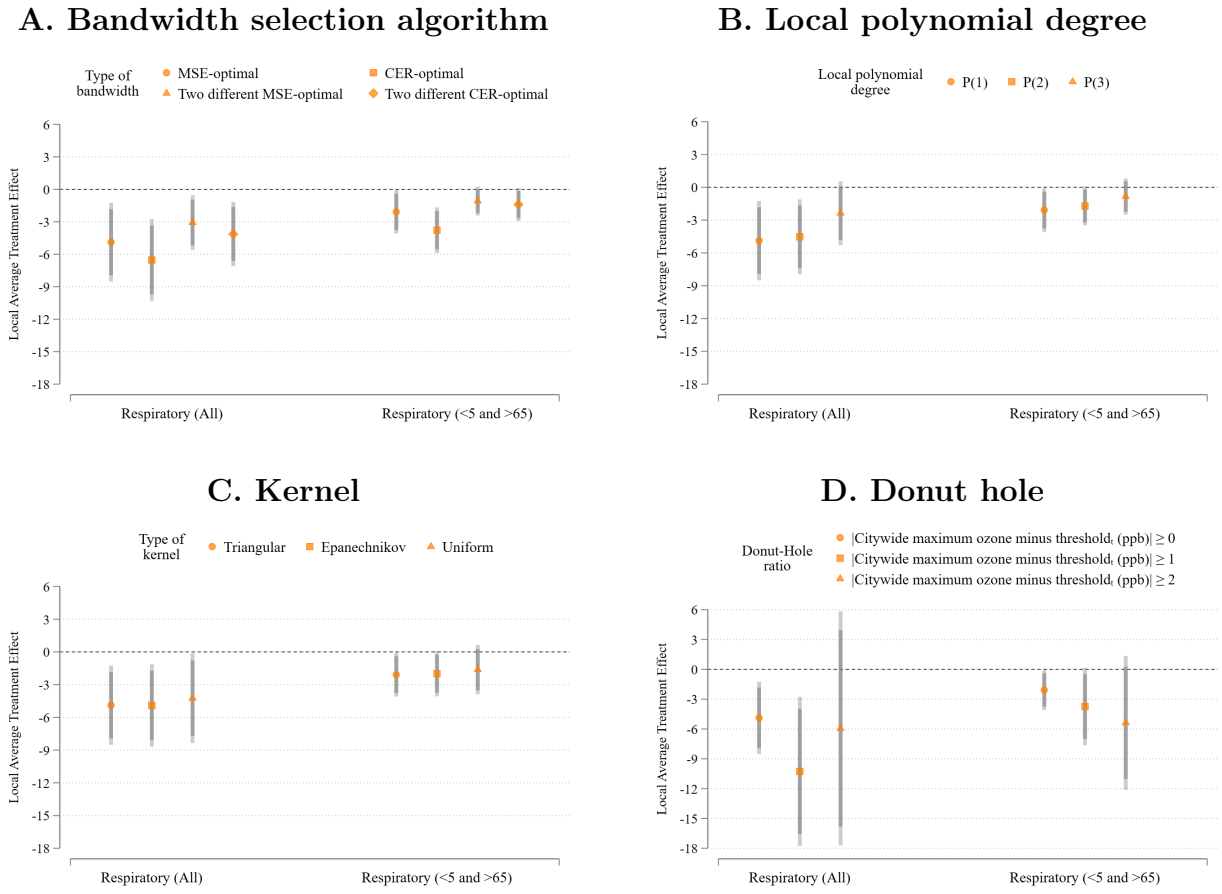

Note: All panels show local average treatment effect (LATE) estimates under different specifications. Panel A shows how the LATE varies with bandwidth selection algorithms, Panel B focuses on changes based on the degree of the local polynomial, and Panel C examines the effect of different kernel choices. Panel D illustrates the robustness of the estimates when I run a donut hole fuzzy regression discontinuity with varying radii. All estimates are calculated with the `rdrobust` package by Calonico et al. (2017). The figure shows 90% (dark gray) and 95% (light gray) confidence intervals for the estimated LATE, obtained with robust bias correction following Calonico et al. (2019). A vector of contemporaneous weather variables is included as a control in all specifications.

To further validate the FRD design employed, I conduct a falsification exercise focusing on the health outcomes. I leverage the fact that acute pollution exposure is expected to impact only a subset of health outcomes, which encompass respiratory and CVD diagnoses (Aguilar-Gomez and Rivera, 2024). Consistent with this expectation, Table 7 shows no statistically significant reductions in ED admissions for digestive conditions, which are relatively common in the dataset, or for cancer diagnoses, which are comparatively rare.

Table 7: **Placebo tests for health outcomes**

	Digestive (All)	Digestive (<5 and >65)	Cancer (All)	Cancer (<5 and >65)
	(1)	(2)	(3)	(4)
Panel A. First Stage	0.730	0.739	0.730	0.725
p-value	$p < 0.001$	$p < 0.001$	$p < 0.001$	$p < 0.001$
CI 95%	[0.68;0.78]	[0.69;0.79]	[0.68;0.78]	[0.67;0.78]
Panel B. ITT	-1.485	-0.418	-0.092	-0.051
p-value	0.141	0.122	0.310	0.129
CI 95%	[-3.46;0.49]	[-0.95;0.11]	[-0.27;0.09]	[-0.12;0.01]
Control Mean	7.369	1.303	0.157	0.029
Panel C. LATE	-2.035	-0.566	-0.127	-0.070
p-value	0.144	0.125	0.314	0.133
CI 95%	[-4.77;0.70]	[-1.29;0.16]	[-0.37;0.12]	[-0.16;0.02]
Bandwidth	5.1	5.0	5.1	5.2
Obs(left|right)	504|360	384|336	504|360	504|360

Note: Panels A and B present estimates of Equation (1) derived with a triangular kernel, a local linear polynomial, and an optimal bandwidth h_{MSE}. In Panel A, the dependent variable is a dummy variable indicating whether the alert is active. In Panel B, the control mean corresponds to the left-hand-side prediction of the nonparametric regression at the threshold. Panel C reports the local average treatment effect (LATE) calculated as the ratio of the intention-to-treat (ITT) effect to the first-stage estimate. All estimates are obtained with the `rdrobust` package by Calonico et al. (2017). The reported coefficients, p-values, and 95% confidence intervals are computed with robust bias correction, following the approach of Calonico et al. (2019). All estimates include a vector of meteorological controls.

8 Discussion

Disorganized urban development across the Global South has often led to high proximity between residential areas and industrial zones. Consequently, many cities in low- and middle-income countries now routinely experience extreme pollution levels, with severe repercussions for human health and productivity (Aguilar-Gomez and Rivera, 2024). In many such contexts, governments have also historically favored a car-focused development approach that, in the long run, produced acute traffic congestion and substantial emissions from mobile sources. In these cities, governments have found themselves faced with a trade-off between the economic activity that keeps the city moving and the health of their population. In the long run, cleaner fleets and abatement technology are the solution; in the short run, air quality warnings and their associated temporary restrictions are part of the policy arsenal

of many of the world's largest metropolises.

Mexico City introduced threshold-based alerts in the mid-1990s, well before comparable programs were launched in Beijing or Delhi, but the system became binding only after a 2016 reform that lowered the ozone trigger to 155 ppb. This long institutional evolution, coupled with a threshold that became binding only recently, makes the PCAA a policy-relevant prototype for megacities now confronting similar extremes. This paper provides robust evidence that the PCAA improves both environmental and health outcomes. An FRD shows substantial same-day drops in ozone and SO_2, mostly driven by enforced cuts at industrial facilities. Respiratory ED visits fall by 41–56%, with larger percentage gains for children and older adults. Google search analytics reveal heightened interest in the alert itself but little evidence of queries related to masks or symptoms, implying that behavioral avoidance is limited. Thus, the data point to mitigation, rather than adaptation, as the dominant short-term mechanism for the effects.

A second reason this setting offers broad policy lessons lies in the city's structure: Its industry and population are tightly co-located, a configuration shared by Jakarta, Delhi, Santiago, and major African hubs such as Lagos and Cairo, where stationary sources of emissions account for a sizable share of SO_2 and primary PM emissions (Sahu et al., 2023; Lestari et al., 2020; Barraza et al., 2017; Clean Air Fund, 2025b,a). The PCAA's cross-jurisdiction governance through CAMe, which initially covered 18 State of Mexico municipalities in addition to the city's own subdivisions,[20] further illustrates how regional cooperation can internalize transboundary externalities in large urban agglomerations.

The results also refine the debate on driving restrictions. Temporary bans cut vehicle counts by approximately 25% yet can raise morning NO_x and CO under VOC-limited conditions—an outcome that complements the long-run substitution effects (second-car purchases) documented by Davis (2008) and Gallego et al. (2013). Policymakers weighing traffic-only measures should therefore consider atmospheric chemistry and potential rebound channels.

Beyond the findings themselves, the study underscores the value of a rich data ecosystem—still a work in progress for many cities in the Global South. Mexico City's dense monitoring network (SIMAT), plant-level emissions reporting (RETC), anonymized ED microdata, and over 300 traffic sensors enabled credible causal evaluation. Few African or Asian megacities currently maintain such integrated datasets; building them will be a step toward advancing

[20] As of 2025, CAMe coordinates air quality policy across six states and more than 80 municipalities in the Mexico City metropolitan area.

evidence-based environmental management.

References

Aguilar-Gomez, S., Dwyer, H., Graff Zivin, J., and Neidell, M. (2022). This is air: The "nonhealth" effects of air pollution. Annual Review of Resource Economics, 14:403–425.

Aguilar-Gomez, S. and Rivera, N. M. (2024). Air pollution in the global south: An overview of its sources and impacts. Serie de Documentos de Trabajo SDT, 561.

Anugerah, A. R., Muttaqin, P. S., and Purnama, D. A. (2021). Effect of large-scale social restriction (PSBB) during COVID-19 on outdoor air quality: Evidence from five cities in DKI Jakarta Province, Indonesia. Environmental Research, 197:111164.

Barraza, F., Lambert, F., Jorquera, H., Villalobos, A. M., and Gallardo, L. (2017). Temporal evolution of main ambient $PM_{2.5}$ sources in Santiago, Chile, from 1998 to 2012. Atmospheric Chemistry and Physics, 17(16):10093–10107.

Brink, L. L., Marshall, L. P., Hacker, K. A., and Talbott, E. O. (2019). Changes in emergency department visits for respiratory and cardiovascular disease after closure of a coking operation near Pittsburgh, PA. Journal of Air Pollution and Health, 4(4):209–220.

Calonico, S., Cattaneo, M. D., Farrell, M. H., and Titiunik, R. (2017). Rdrobust: Software for regression-discontinuity designs. The Stata Journal, 17(2):372–404.

Calonico, S., Cattaneo, M. D., Farrell, M. H., and Titiunik, R. (2019). Regression discontinuity designs using covariates. Review of Economics and Statistics, 101(3):442–451.

Calonico, S., Cattaneo, M. D., and Titiunik, R. (2014). Robust nonparametric confidence intervals for regression-discontinuity designs. Econometrica, 82(6):2295–2326.

Calonico, S., Cattaneo, M. D., and Titiunik, R. (2015). Optimal data-driven regression discontinuity plots. Journal of the American Statistical Association, 110(512):1753–1769.

CAQM (2022). Revised graded response action plan (GRAP) for ncr, commission for air quality management in national capital region and adjoining areas CAQM.

CAQM (2023). Graded Response Action Plan (GRAP) for NCR – Revised Schedule (October 2023), Commission for Air Quality Management (CAQM). Official PDF document. Comprehensively revised GRAP schedule for stages I–IV.

Cattaneo, M. D., Idrobo, N., and Titiunik, R. (2019). A practical introduction to regression discontinuity designs: Foundations. Cambridge University Press.

Chen, X., Shen, X., and Zhuge, A. (2024). Pollution matters: The political cost of information disclosure. Governance, 37(4):1275–1297.

Cheng, N., Zhang, D., Li, Y., Xie, X., Chen, Z., Meng, F., Gao, B., and He, B. (2017). Spatio-temporal variations of $PM_{2.5}$ concentrations and the evaluation of emission reduction measures during two red air pollution alerts in Beijing. Scientific Reports, 7(1).

Clean Air Fund (2025a). Clean air factsheet: Cairo. https://www.cleanairfund.org/resource/clean-air-factsheet-cairo/. Accessed: 9 July 2025.

Clean Air Fund (2025b). Clean air factsheet: Lagos. https://www.cleanairfund.org/resource/clean-air-factsheet-lagos/. Accessed: 2025-07-01.

Cook, C., Kreidieh, A., Vasserman, S., Allcott, H., Arora, N., van Sambeek, F., Tomkins, A., and Turkel, E. (2025). The short-run effects of congestion pricing in New York City. Technical report, National Bureau of Economic Research.

Dangel, A. and Goeschl, T. (2025). Air quality alerts and don't drive appeals: Evidence on voluntary pollution mitigation dynamics from Germany.

Davis, L. W. (2008). The effect of driving restrictions on air quality in Mexico City. Journal of Political Economy, 116(1):38–81.

Dong, Y. (2018). Alternative assumptions to identify late in fuzzy regression discontinuity designs. Oxford Bulletin of Economics and Statistics, 80(5):1020–1027.

El Poder del Consumidor (2010). Calidad del transporte público en el Distrito Federal. Accessed: February 1, 2025.

Fan, M., Jiang, H., and Zhou, M. (2023). Beyond particulate matter: New evidence on the causal effects of air pollution on mortality. Journal of Health Economics, 91.

Gallego, F., Montero, J.-P., and Salas, C. (2013). The effect of transport policies on car use: Evidence from Latin American cities. Journal of Public Economics, 107:47–62.

GDF (2016). Gaceta oficial de la Ciudad de México, Gobierno del Distrito Federal (GDF). Décima novena época. https://data.consejeria.cdmx.gob.mx/portal_old/uploads/gacetas/502c558a02ee0f216ed018e9acc6b4ec.pdf. Accessed: July 3, 2025.

Guevara, M., Enciso, S., Tena, C., Jorba, O., Dellaert, S., Denier van der Gon, H., and Pérez García-Pando, C. (2024). A global catalogue of CO_2 emissions and co-emitted species from power plants, including high-resolution vertical and temporal profiles. Earth System Science Data, 16:337–373.

Hahn, J., Todd, P., and Van der Klaauw, W. (2001). Identification and estimation of treatment effects with a regression-discontinuity design. Econometrica, 69(1):201–209.

INFOCDMX (2023). Análisis de la información disponible sobre el sistema de movilidad en la Ciudad de México. Accessed: January 31, 2025.

International Energy Agency (2024). Global ev outlook 2024. Technical report, IEA, Paris. Licence: CC BY 4.0.

Juan Lopez, M., Martinez Valle, A., and Aguilera, N. (2015). Reforming the Mexican health system to achieve effective health care coverage. Health Systems & Reform, 1(3):181–188.

Lestari, P., Damayanti, S., and Arrohman, M. K. (2020). Emission inventory of pollutants (CO, SO_2, $PM_{2.5}$, and NO_X) in Jakarta Indonesia. In IOP conference series: Earth and environmental science, volume 489. IOP Publishing.

Li, J., Irfan, M., Samad, S., Ali, B., Zhang, Y., Badulescu, D., and Badulescu, A. (2023a). The relationship between energy consumption, CO_2 emissions, economic growth, and health indicators. International Journal of Environmental Research and Public Health, 20(3).

Li, X., Yao, Y., Zhang, Z., Zeng, Z., Chen, Z., and Du, H. (2023b). The health and economic impacts of emergency measures to combat heavy air pollution. Journal of Cleaner Production, 423.

Lin, C.-Y. C. (2010). A spatial econometric approach to measuring pollution externalities: An application to ozone smog. Journal of Regional Analysis & Policy, 40(1):1–19.

Lin, C.-Y. C., Zhang, W., and Umanskaya, V. I. (2011). The effects of driving restrictions on air quality: São Paulo, Bogotá, Beijing, and Tianjin. Technical report.

McCrary, J. (2008). Manipulation of the running variable in the regression discontinuity design: A density test. Journal of econometrics, 142(2):698–714.

Mullins, J. and Bharadwaj, P. (2015). Effects of short-term measures to curb air pollution: evidence from Santiago, Chile. American Journal of Agricultural Economics, 97(4):1107–1134.

Neidell, M. (2009). Information, avoidance behavior, and health the effect of ozone on asthma hospitalizations. Journal of Human resources, 44(2):450–478.

OECD (2014). Guidance document on elements of a PRTR: Part 1. OECD Series on prevention and control of pollutant releases. OECD Publishing, Paris.

OECD (2016). The economic consequences of outdoor air pollution. Technical report, Paris.

Redacción Obras (2025). Zmvm: El contraste del transporte público entre el centro y la periferia. Obras.

Rivera, N. M. (2021). Air quality warnings and temporary driving bans: Evidence from air pollution, car trips, and mass-transit ridership in Santiago. Journal of Environmental Economics and Management, 108.

Saberian, S., Heyes, A., and Rivers, N. (2017). Alerts work! Air quality warnings and cycling. Resource and Energy Economics, 49:165–185.

Sahu, S. K., Mangaraj, P., and Beig, G. (2023). Decadal growth in emission load of major air pollutants in Delhi. Earth System Science Data, 15:3183–3202.

Schlenker, W. and Walker, W. R. (2016). Airports, air pollution, and contemporaneous health. Review of Economic Studies, 83(2):768–809.

SEDEMA (2018). Registro de emisiones y transferencia de contaminantes de la Ciudad de México 2016, Secretaría del Medio Ambiente de la Ciudad de México (SEDEMA). https://www.sedema.cdmx.gob.mx/storage/app/media/DGEIRA/registrosambientales/RETC/RETC2016.pdf. Accessed: July 3, 2025.

SEMOVI (2019). Programa integral de movilidad 2019-2024, Secretaría de Movilidad de la Ciudad de México (SEMOVI). Accessed: January 31, 2025.

Singh, Y. and Kulshrestha, U. (2020). An analysis of GRAP task force directions for improved AQI in Delhi during 2018. Current World Environment, 15:29–41.

Smith, S. J., van Aardenne, J., Klimont, Z., Andres, R. J., Volke, A., and Delgado Arias, S. (2011). Anthropogenic sulfur dioxide emissions: 1850–2005. Atmospheric Chemistry and Physics, 11:1101–1116.

Tribby, C. P., Miller, H. J., Song, Y., and Smith, K. R. (2013). Do air quality alerts reduce traffic? An analysis of traffic data from the Salt Lake City metropolitan area, Utah, USA. Transport Policy, 30:173–185.

Viard, V. B. and Fu, S. (2015). The effect of Beijing's driving restrictions on pollution and economic activity. Journal of Public Economics, 125:98–115.

Welch, E., Gu, X., and Kramer, L. (2005). The effects of ozone action day public advisories on train ridership in Chicago. Transportation Research Part D: Transport and Environment, 10(6):445–458.

WHO (2021). Who global air quality guidelines.

Winick, R. M., Matherly, D., and Ismart, D. (2008). potential for reductions in discretionary travel during peak periods. (FHWA-HOP-09-017).

World Health Organization (2021). Who global air quality guidelines. Ozone (O_3) peak-season 8-h mean: 100 µg/m^3 $\approx$ 50 ppb.

World Health Organization (2024). Ambient (outdoor) air quality and health. WHO website. Accessed: February 1, 2025.

Yao, Y., Li, X., Smyth, R., and Zhang, L. (2022). Air pollution and political trust in local government: Evidence from China. Journal of Environmental Economics and Management, 115.

Zhang, W., Lawell, C.-Y. C. L., and Umanskaya, V. I. (2017). The effects of license plate-based driving restrictions on air quality: Theory and empirical evidence. Journal of Environmental Economics and Management, 82:181–220.

Online Appendix

Table A.1: **PCAA – Measures**

	Measures
General Public	**Recommendations** Reduce the time spent outdoors Reduce liquefied petroleum gas (LPG) consumption Report fires and gas leaks to the corresponding authorities Carpooling and home office are recommended **Mandatory actions or restrictions** Suspend outdoor activities in all schools
Transport	No vehicles for publicity purposes Additional age- and emissions-based driving restrictions are added to the HNC
Industry	Suspend activities that generate fugitive emissions from VOC Suspend activities in establishments that use wood or coal Suspend all construction, remodeling, demolition and movement activities Stop operation at gasoline stations that do not have return systems for petrol fumes Suspend printing activities using VOCs without emission control systems Suspend industrial activities using benzene, toluene, xylene or derivatives without control equipment Suspend cleaning and degreasing processes with uncontrolled VOC emissions Fixed sources in the manufacturing industry with combustion processes must reduce emissions by 30–40% from baseline during the alert Exempted fixed sources in the manufacturing industry must reduce NO_x emissions by an additional 30% from day 4 of the alert Thermoelectric plants must reduce operations by 50% during the alert LPG storage and distribution plants must suspend maintenance, repair and transfer operations
Authorities	Suspend infrastructure maintenance, including paving Strengthen the monitoring and combat of fires in agricultural and forest areas Strengthen the surveillance and fines of vehicles and establishments who fail to comply with the respective measures Suspend activities that involve ceramic or brick baking and melting furnace

Note: The table summarizes the most relevant measures of the Mexico City Environmental Alerts Program (PCAA). In 2016, prewarnings were eliminated from the program, and all measures listed in Panel 1 of the table were incorporated into Phase 1. The table is based on information from the official *Mexico City Gazettes*, available online. For the purposes of this paper, I focus on post-reform alerts to examine the impacts of the policy with driving restrictions. *Precontingencia* and Phase II measures are not included in the table because they were never activated during the analysis period.

Figure A.1: **Timing of restrictions: Example from alert issued on August 7, 2016**

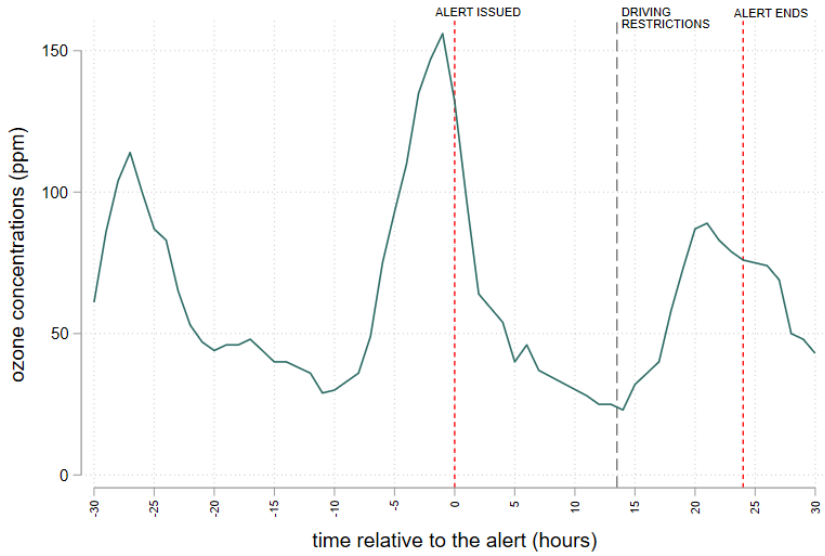

Note: The figure shows the trajectory of ozone (O_3) in the 48 hours before and after the Mexico City Environmental Alerts Program (PCAA) alert issued on August 7, 2016. The line represents the hourly average of monitor-level readings.

Figure A.2: **Histogram of alerts since 2016 by duration**

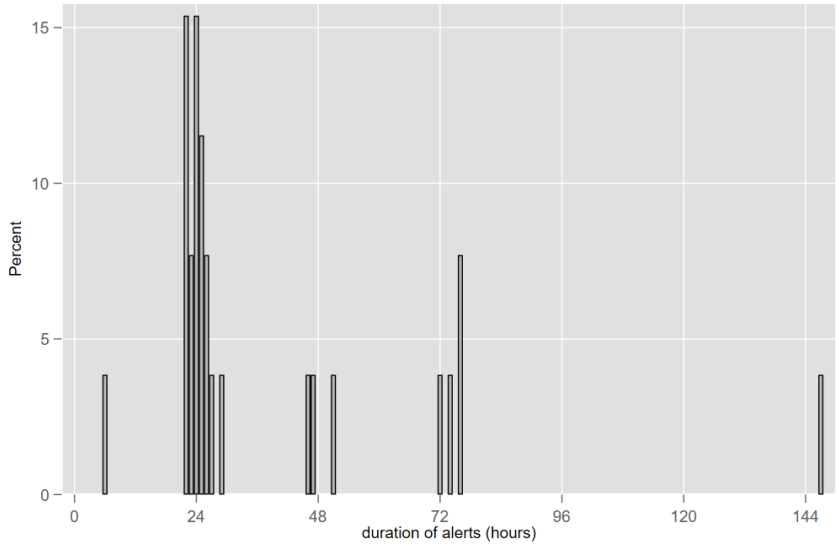

Note: The figure shows the distribution of alerts by their duration, measured in hours between activation and deactivation. Source: Atmospheric Monitoring System (SIMAT).

Figure A.3: **Traffic data**

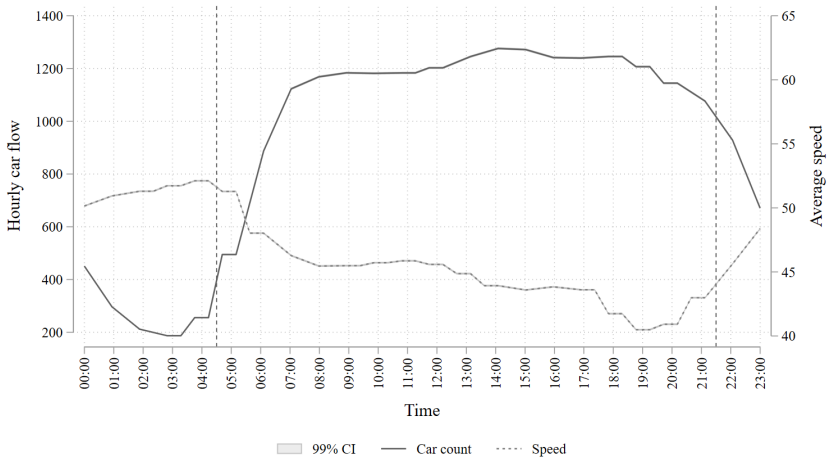

Note: The figure displays hourly speed and flow averages. Observations are collected from 343 monitors in the city. Speed is measured in km/h, and flow in cars is counted per hour. Data are from the Mexico City Open Data Portal.

Figure A.4: **Interest over time**

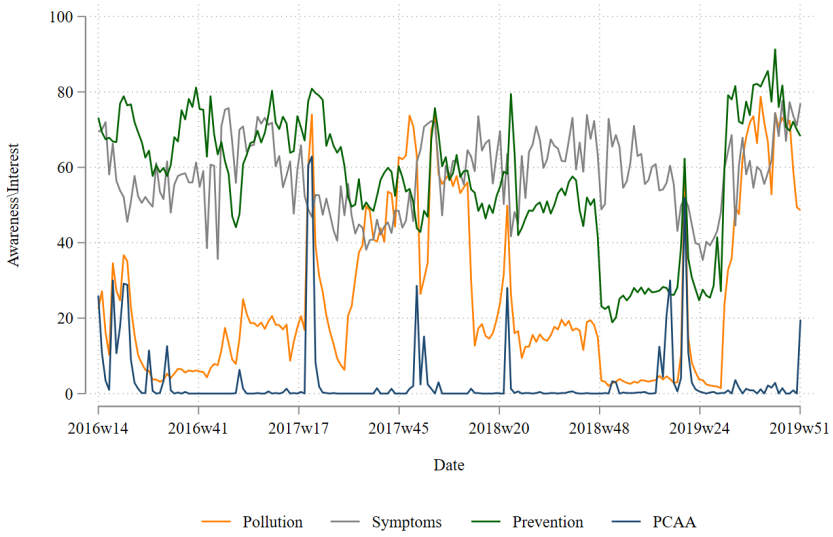

Note: The figure shows the evolution of weekly search interest in Mexico City for four categories of terms related to air quality: *pollution* (e.g., "smog," "ozone"), *symptoms* (e.g., "asthma," "irritated eyes"), *prevention* (e.g., "face mask," "air purifier"), and *PCAA* (e.g., "environmental contingency," "Phase 1"). The indicators are constructed from Google Trends data and standardized on a 0–100 scale, where 100 represents the week with the highest search interest in the category. Each line represents the weekly average of the search index across terms within the category.

Table A.2: **Search terms used to construct Google Trends indicators by category**

Category	Search Terms	Query List
Pollution	Original	contaminacion + smog + ozono + imeca + calidad del aire + contaminacion ambiental
	Translated	pollution + smog + ozone + IMECA + air quality + environmental pollution
Symptoms	Original	asma + alergia + ojos irritados + problemas respiratorios
	Translated	asthma + allergy + irritated eyes + respiratory problems
Prevention	Original	prevencion + exposicion al aire + mascarilla + filtro + purificador de aire + cubrebocas
	Translated	prevention + air exposure + face mask + filter + air purifier + face covering
PCAA	Original	contingencia ambiental + alerta ambiental + fase 1 + fase 2 + semaforo ambiental + programa PCAA
	Translated	environmental contingency + environmental alert + phase 1 + phase 2 + environmental traffic light + PCAA program

Note: This table lists the search terms used to construct the Google Trends indicators for each thematic category. Terms were originally selected in Spanish and translated into English for reference. Each indicator reflects the daily search interest averaged across all terms in the category, based on data for Mexico City from April 1, 2016 to December 31, 2019.

Table A.3: **Descriptive statistics**

	Obs	Mean	Std Dev	Min	Max
a) Pollution					
O_3 (*ppb*)	32,784	30.31	24.57	0.84	132.35
SO_2 (*ppb*)	32,784	3.98	5.34	0.3	80.74
CO (*ppm*)	32,784	0.5	0.31	0.02	2.56
NO_x (*ppb*)	32,784	39	27.26	3.4	234.42
PM_{10} ($\mu g/m^3$)	32,784	42.53	21.25	3.17	223.75
b) Traffic					
Average speed (km/h)	29,109	47.37	7.19	8.13	133.15
Number of cars	29,832	290,286.55	142,567.93	0	891,540
Number of trucks	29,832	21,564.34	24,929.91	0	661,676
Number of buses	29,832	26,515.36	21,847.52	0	244,610
Number of small buses/vans	29,832	114,468.33	71,932.18	0	2,193,264
c) Hourly ED visits					
Respiratory (All)	32,783	11.58	9.53	0	116
Respiratory (<5 and >65)	32,783	5.89	5.3	0	71
CVD (All)	32,783	3.14	3.31	0	42
CVD (<5 and >65)	32,783	1.03	1.37	0	20
d) Awareness					
Pollution	1,366	25.56	23.88	0	100
Symptoms	1,366	57.91	16.07	0	100
Prevention	1,366	56.88	18.97	12	100
PCAA	1,366	3.25	12.40	0	100

Note: This table presents the main descriptive statistics for different variables. Panel a) shows pollution statistics, where observations are at the hour level. Panel b) includes traffic data, where observations are at the hour level. Panel c) reports health outcomes, with observations at the hour level. Panel d) contains awareness indices constructed from Google Trends data, aggregated at the daily level. These indices capture relative search interest in four topics: *pollution*, *symptoms*, *prevention*, and *PCAA*. Each index is normalized from 0 to 100 and reflects the popularity of grouped search terms over time in Mexico City. The data cover the period from April 4, 2016, to December 31, 2019.

Table A.4: **ITT effect on pollution**

	Probability of Alert Activation
	(1)
Panel A. First Stage	0.518
p-value	$p < 0.001$
CI 95 percent	[0.236;0.799]
Bandwidth	17.79
Obs(left|right)	78 | 25

Note: All estimates include a vector of covariates **X**, which incorporates current climate variables. Panels A present estimates of Equation (1) derived with a triangular kernel, a local linear polynomial, and an optimal bandwidth h_{MSE}. In Panel A, the dependent variable is a dummy variable indicating whether the alert is active. All estimates are obtained with the `rdrobust` package by Calonico et al. (2017). The reported coefficients, p-values, and 95% confidence intervals are computed with robust bias correction, following the approach of Calonico et al. (2019).

Table A.5: **Temporal heterogeneity in traffic response to PCAA alerts**

Older alerts	Congestion (average speed)	Cars	Trucks (hourly vehicle trips)	Buses	Pesero-vans
	(1)	(2)	(3)	(4)	(6)
Panel A. First Stage	0.860	0.818	0.817	0.839	0.815
p-value	$p < 0.001$	$p < 0.001$	$p < 0.001$	$p < 0.001$	$p < 0.001$
CI 95%	[0.81;0.91]	[0.77;0.86]	[0.77;0.86]	[0.79;0.89]	[0.77;0.86]
Panel B. ITT	-.541	-13,298	-13,673	-15,850	-37,301
p-value	0.386	0.466	0.007	0.007	0.056
CI 95%	[-1.76;.681]	[-49,031;22,436]	[-23,692;-3,653]	[-27,393;-4,307]	[-75,606;10,03]
Control Mean	50.4	228555	41873	47484	127068
Panel C. LATE	-.643	-16,258	-16,759	-18,894	-45,474
p-value	0.390	0.477	0.009	0.008	0.070
CI 95%	[-2.11;.822]	[-61016;28501]	[-29,381;-4,138]	[-32,900;-48,88]	[-94,648;3,701]
Bandwidth	4.4	5.4	5.3	4.4	6.4
Obs(left|right)	192|168	240|192	240|192	192|168	288|216
Recent Alerts	Congestion (average speed)	Cars	Trucks (hourly vehicle trips)	Buses	*Pesero* vans
	(1)	(2)	(3)	(4)	(6)
ITT	13	-197,257	-20,623	-26,966	-102,459
p-value	$p < 0.001$	$p < 0.001$	$p < 0.001$	$p < 0.001$	$p < 0.001$
CI 95%	[10.4;15.5]	[-298,311;-96,203]	[-24,722;-16,523]	[-33,376;-20,557]	[-139,820;-65,098]
Control Mean	45.9	32,5607	15,272	20,495	118,565
Bandwidth	4.7	5.4	4.9	5.1	4.1
Obs(left|right)	144|120	216|120	144|120	216|120	144|120

Note: All estimates include a vector of covariates $\mathbf{X}$, which incorporates contemporaneous weather variables. Panels A and B present estimates of Equation (1) derived with a triangular kernel, a local linear polynomial, and an optimal bandwidth h_{MSE}. In Panel A, the dependent variable is a dummy variable indicating whether the alert is active. In Panel B, the control mean corresponds to the left-hand-side prediction of the nonparametric regression at the threshold. Panel C reports the local average treatment effect (LATE) calculated as the ratio of the intention-to-treat (ITT) effect to the first-stage estimate. Older alerts include the first third of the sample and recent alerts the last third. For recent alerts, I employ a sharp regression discontinuity design because there is perfect compliance in the first stage. All estimates are obtained with the `rdrobust` package by Calonico et al. (2017). The reported coefficients, *p*-values, and 95% confidence intervals are computed with robust bias correction, following the approach of Calonico et al. (2019).

Table A.6: **Impacts of PCAA alerts on information-seeking behavior**

	Pollution	Symptoms	Prevention	PCAA
	(1)	(2)	(3)	(4)
Panel A. First Stage	0.532	0.527	0.508	0.509
p-value	$p < 0.001$	$p < 0.001$	$p < 0.001$	$p < 0.001$
CI 95 percent	[0.24;0.82]	[0.24;0.82]	[0.24;0.77]	[0.23;0.79]
Panel B. ITT	-0.604	-10.571	8.467	16.140
p-value	0.949	0.113	0.315	0.265
CI 95 percent	[-19.219;18.010]	[-23.654;2.513]	[-8.049;24.984]	[-12.239;44.520]
Control Mean	3.735	58.049	45.284	-8.929
Panel C. LATE	-1.060	-19.960	16.529	32.067
p-value	0.951	0.161	0.326	0.145
CI 95 percent	[-34.844;32.725]	[-47.881;7.961]	[-16.478;49.536]	[-11.105;75.239]
Bandwidth	12.1	12.8	18.2	15.0
Obs(left|right)	51|20	51|20	91|25	64|24

Note: All estimates include a vector of covariates $\mathbf{X}$, which incorporates contemporaneous weather variables. Panels A and B present estimates of Equation (1) derived with a triangular kernel, a local linear polynomial, and an optimal bandwidth h_{MSE}. In Panel A, the dependent variable is a dummy variable indicating whether the alert is active. In Panel B, the control mean corresponds to the left-hand-side prediction of the nonparametric regression at the threshold. Panel C reports the local average treatment effect (LATE) calculated as the ratio of the intention-to-treat (ITT) effect to the first-stage estimate. All estimates are obtained with the `rdrobust` package by Calonico et al. (2017). The reported coefficients, p-values, and 95% confidence intervals are computed with robust bias correction, following the approach of Calonico et al. (2019).

Figure A.5: **Heterogeneity by treatment intensity, all industries**

A. Monitor-level SO_2 and nearby industrial pollution – full sample

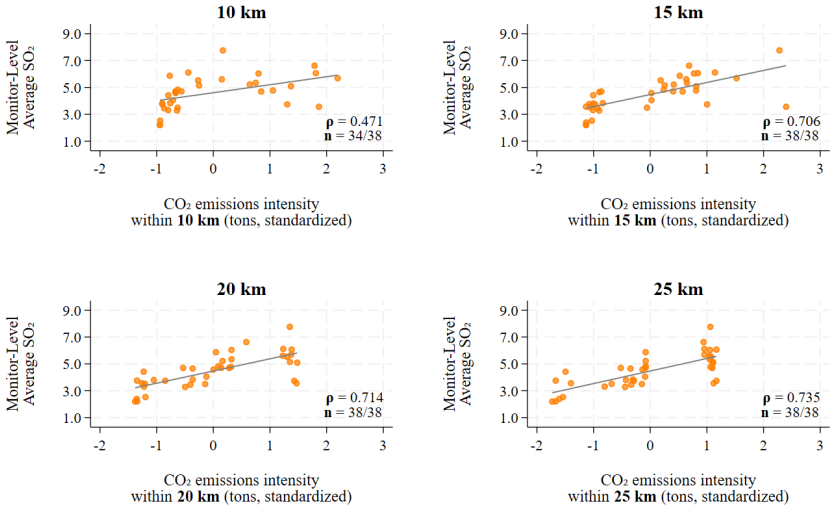

B. RD estimates by industrial emissions intensity

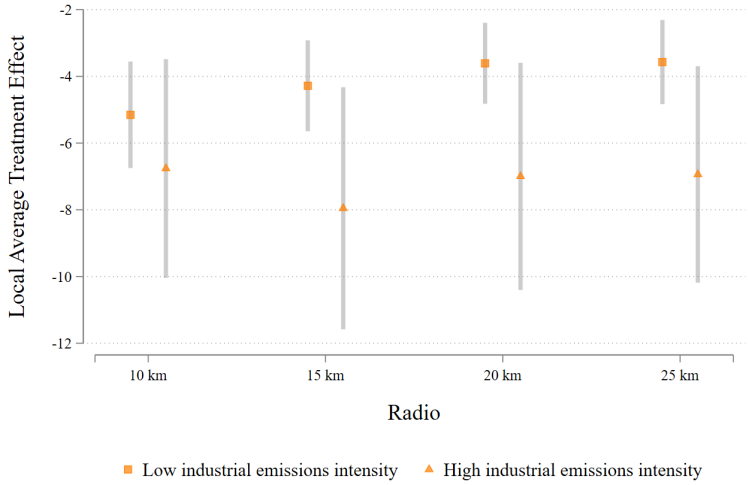

Note: Each scatterplot in Panel A shows the correlation between the average SO_2 concentration recorded at each monitoring station (y-axis) and the intensity of nearby industrial CO_2 emissions within 10, 15, 20, and 25 km (x-axis). The value of ρ denotes the Pearson correlation coefficient. The value of n indicates the number of monitoring stations with at least one facility located within the corresponding radius. All industries are included, regardless of whether they are subject to Mexico City Environmental Alerts Program (PCAA) restrictions. A linear fit is included to guide interpretation. In Panel B, the plotted coefficients correspond to local average treatment effects (LATEs) estimated via a fuzzy regression discontinuity design using the ozone threshold rule, based on Equation (1). Vertical bars show 95% confidence intervals.

Table A.7: **Restricted Industries**

NAICS Code	Industry	Sector	Number of plants	Aggregate CO_2 emissions
325999	Manufacture of other chemicals	Chemistry	6	771,908
221110	Electric power generation, transmission, and distribution	Electric Power Generation	11	582,946
322299	Manufacture of other paperboard and paper products	Cellulose and paper	4	302,819
322121	Papermaking in integrated plants	Cellulose and paper	2	107,278
339999	Other manufacturing industries	Wood & products	11	83,992
332720	Manufacture of screws, nuts, rivets and the like	Metallurgical (includes steel)	2	67,221
331520	Casting of nonferrous metal parts	Metallurgical (includes steel)	2	46,889
325610	Manufacture of soaps, cleaners and toothpastes	Chemistry	6	45,363
221120	Electric power transmission and distribution	Electric power generation	1	44,871
325412	Manufacture of pharmaceutical preparations	Chemistry	21	41,815
311422	Fruit & veg. preservation (nonfreezing/dehydration)	Food & bev. (human use)	1	39,630
322132	Manufacture of cardboard and cardboard from pulp	Cellulose and paper	2	36,523
311222	Manufacture of edible vegetable oils and fats	Chemistry	1	31,522
314999	Flag & Misc. Textile Mfg. (n.e.c.)	Textiles, fibers and yarns	1	21,555
325411	Manufacture of raw materials for the pharmaceutical industry	Chemistry	3	17,702
311110	Animal feed processing	Other	1	15,677
325180	Manufacture of other inorganic basic chemicals	Chemistry	4	15,641
331420	Secondary copper rolling	Metallurgical (includes steel)	1	15,288
336330	Auto steering & suspension parts mfg.	Automotive	1	15,087
323119	Continuous shape printing and other prints	Other	2	9,633
326211	Manufacture of rims and tubes	Automotive	3	8,863
336120	Truck and tractor trailer manufacturing	Automotive	1	7,836
322210	Carton packaging manufacturing	Cellulose and paper	3	7174
327999	Manufacture of products from nonmetallic minerals	Metallurgical (includes steel)	2	6,668
311999	Processing of other foods	Food & bev. (human use)	1	5,676
325211	Manufacture of synthetic resins	Chemistry	7	5,182
332110	Manufacture of forged and die-cut metal products	Metal articles & products	1	4,510
325520	Adhesive manufacturing	Chemistry	3	4,488
336390	Manufacture of other parts for automotive vehicles	Automotive	2	4,365
326290	Manufacture of other rubber products	Chemistry	5	3,879
325130	Manufacture of synthetic pigments and dyes	Chemistry	1	3,502
332610	Manufacture of wire, wire products and springs	Metal articles & products	1	3,019
326150	Manufacture of urethane foams and products	Chemistry	1	2,543
541990	Other professional, scientific and technical services	Chemistry	1	2,138
325310	Fertilizer manufacturing	Chemistry	1	2119
326220	Manufacture of rubber and plastic belts and hoses	Chemistry	1	1,989
551111	Corporate	automotive	1	1,628
325190	Manufacture of other organic basic chemicals	Chemistry	1	1,401
325510	Paint and coatings manufacturing	Paints and inks	3	1,238
332999	Manufacture of other metal products	Elec., electr. & HH equip.	2	991
339112	Manufacture of disposable material for medical use	Chemistry	1	853
325212	Manufacture of synthetic rubbers	Chemistry	1	828
325910	Printing ink manufacturing	Paints and inks	1	721
326110	Manufacture of flexible plastic bags and films	Plastic articles & products	1	697
332510	Hardware and lock manufacturing	Metal articles & products	1	640
336340	Manufacture of brake system parts for automotive vehicles	Automotive	1	630
325620	Manufacture of cosmetics, perfumes, etc.	Chemistry	2	559
336370	Manufacture of die-cut metal parts for automotive vehicles	Automotive	1	548
323120	Printing-related industries	Other	1	392
327910	Manufacture of abrasive products	Metallurgical (includes steel)	1	344
331220	Manufacture of other iron and steel products	Metallurgical (includes steel)	2	311
324191	Manufacture of lubricating oils and greases	Chemistry	1	292
521110	Central banking	Other	1	236
331510	Casting molding of iron and steel parts	Metallurgical (includes steel)	1	232
333412	Refrigeration equipment manufacturing	Metallurgical (includes steel)	1	223
313310	Textile product finishing	Textiles, fibers and yarns	1	222
335311	Manufacture of electric motors and generators	Elec., electr. & HH equip.	1	168
325320	Manufacture of pesticides and agrochemicals, except fertilizers	Chemistry	1	158
331310	Basic aluminum industry	Metallurgical (includes steel)	1	114
331419	Smelting and refining of other nonferrous metals	Metallurgical (includes steel)	1	101

Note: This list includes the manufacturing subsectors subject to activity restrictions according to the official regulation published in the *Mexico City Gazettes*, Vol. 19, No. 4, dated February 5, 2016. These restrictions are part of the Mexico City Environmental Alerts Program (PCAA), implemented by the ministry of the environment to control emissions during air pollution contingencies.